FINAL REPORT ON CONTRACT NO. NAS 9-6177

(Phase 2)

DEVELOPMENT OF ELECTROFORMING TECHNIQUES FOR THE FABRICATION OF ROCKET ENGINE INJECTORS

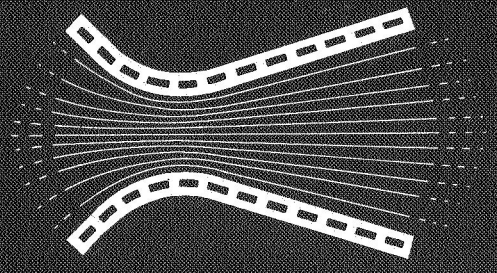

CAMIN LABORATORIES INC.
BROOKLYN, NEW YORK

NASA CR 101801

FINAL REPORT ON CONTRACT NO. NAS 9-6177

(Phase 2)

DEVELOPMENT OF ELECTROFORMING TECHNIQUES FOR THE FABRICATION OF ROCKET ENGINE INJECTORS

Prepared by:

Vito D. Agosta

Sanford S. Hammer
Director of Engineering

Approved:

Samuel Fialkoff
Vice President

CAMIN LABORATORIES, INC.
104-14 South Fourth Street
Brooklyn, New York

APRIL 1969

TABLE OF CONTENTS

LIST OF FIGURES

FOREWORD

This report, which is concerned with demonstrating the feasibility of fabricating injectors by the electroforming process, was prepared by Camin Laboratories, Inc., Brooklyn, New York under NASA Contract NAS 9-6177, Phase 2. Mr. Samuel Fialkoff served as program manager. Dr. Sanford S. Hammer was project engineer and was responsible for the fabrication of the injectors. Dr. Vito D. Agosta designed and prescribed the test procedure for the injectors. The electrochemical aspects of the program were conducted by Mr. Zdenek Cacka.

The program was administered under the direction of the Manned Spacecraft Center, General Research Procurement Branch. The Technical Monitor was Mr. Norman H. Chaffee.

The work reported herein was performed during the period 1 September 1967 to 31 March 1969.

SUMMARY

A program was conducted to demonstrate the feasibility of fabricating injectors by the electroforming process. The scope of this program consisted of designing, fabricating and hydraulically flow testing 100-pound thrust rocket engine injectors for use with hypergolic earth storable bipropellants.

Six conceptual injector designs were generated of which two were selected for fabrication. Four injectors of each configuration were fabricated and subjected to testing in order to demonstrate reproducibility of design and hydraulic characteristics.

The results of the tests include the following information:

(a) The coefficients of discharge for the fuel and oxidant are 0.641 and 0.692, respectively. The maximum propellant flow deviations are within the experimental error for fuel, and within $\pm 5\%$ of the flow band error for the oxidant. The $^{O}/F$ ratios for the eight injectors are in the range $1.88 \leq {}^{O}/F \leq 2.45$ as compared to $1.85 \leq {}^{O}/F \leq 2.50$ determined from the experimental mean value of $^{O}/F = 2.16$ and including the above-mentioned experimental deviations.

(b) Nominal values for fuel and oxidant flow in the precombustion cup are 12.7% and 14.1%, respectively.

These compare with calculated values of 13.0% and 15.5%, respectively. Five out of 128 main orifices show significant deviation in the main flow. Eleven out of 64 film cooling orifices show flow deviation in the .008 in. holes for film cooling. Nine of these are on the low side which indicate partially blocked orifices.

(c) Lag times for the bulk flow are referenced to the appearance of propellant from the precombustion cup. Lag times of zero and 0.011 sec for oxidant and fuel mass flow, respectively, are measured for injectors with swirl cup. These compare with zero and 0.009 predicted theoretically. Lag times of .005 sec and .056 sec for oxidant and fuel mass flow, respectively, are measured for injectors with impinging jets in the precombustion cup. These compare with .007 sec and 0.025 sec predicted theoretically.

The results of this investigation indicate that injectors can be fabricated by the electroformation process. The injectors can include intricate internal flow geometry and can be free of welds, interference fits, brazed joints. Reproducibility of dimensions and hydraulic characteristics is as good as the state-of-the-art injectors manufactured by conventional machining methods.

I. INTRODUCTION

The program described in this report is concerned with demonstrating the feasibility of fabricating injectors by the electroforming process. The scope of this program consists of designing, fabricating and flow testing 100-pound thrust, hypergolic, bipropellant, rocket engine injectors.

A. Background.

Conventional fabrication techniques employed for injector designs that include intricate manifold passages and orifice patterns, consist of welding, bolting, or pressure fitting several sub-assemblies together. This practice imposes constraints in the freedom of injector design, lessens operational reliability, and leads to increased costs. Where drilling operations are involved, the possibility of drill breakage, drill misalignment, and burr formation in enclosed passages results in injectors with different operational characteristics.

It is suggested that the use of electroforming techniques for the fabrication of injectors would minimize the aforementioned disadvantages. In particular, greater design freedom and operational reproducibility and reliability would accrue.

The electroforming process is a method of fabricating intricate parts by the electrodeposition of metal from an electrolytic solution onto a mandrel. After a quantity of the metallic deposit has accumulated on the mandrel, it is possible to remove the

work-piece from the solution and perform standard machining operations. Repetition of this operation allows for the fabrication of intricate structures in one piece.

A method to fabricate injectors by the electroforming process was developed and reported (Contract No. NAS 9-6177, May 15, 1967) by Camin Laboratories, Inc. The process involved the machining of a single master plate which served as a transfer of the final injector face. Holes in the master plate representing the injector orifice layout were fitted with precise disposable pins. A multiplicity of "slaves" or injectors were generated from the master plate by the electroforming process. Internal propellant feed passages and manifolding were generated during the process by interrupting the deposition cycle and incorporating disposable filler materials. Inspection and deburring the orifice inlets were accomplished at these times. The final products were a series of injectors reproduced from a single master, devoid of any welds or brazes.

B. Objective.

The objective of this program is to demonstrate the use of the electroforming process in the fabrication of injectors for 100-pound thrust hypergolic bipropellant rocket engines. Specifically, the program objectives are:

1. Demonstrate that the electroforming process can be used to fabricate injectors of complex internal flow geometry, similar

to current state-of-the-art injectors manufactured by conventional machining techniques.

2. Demonstrate that complex injectors can be manufactured as integral units, free of interface fits, welds, etc., in the regions of the injector face and manifolds.

3. Demonstrate that the use of the electroforming process to fabricate injectors permits increased design flexibility by removing constraints imposed by normal fabrication techniques.

4. Demonstrate the reproducibility of critical dimensions, orifices, etc., and the superior reproducibility of hydraulic characteristics from one unit to another.

C. Program Plan.

This program is divided into two phases, namely:

1. Injector design
2. Injector fabrication and test.

The injector designs should reflect as much as possible the advantages of the electroforming process.

II. INJECTOR DESIGN

The injector design requirements are given below. Six conceptual injector designs were generated for consideration. Subject to NASA approval, two candidate injector designs were selected for fabrication and include the injector orifice patterns, precombustion devices, internal flow passages and provision for fuel film cooling of the chamber internal walls. Upon discussion with NASA, it was decided to design the injector to mate with the Moog Bipropellant Valve Model 52 x 108, and interface with a given combustion chamber.

All critically dimensioned and located components of the injector shall be formed from nickel by the electroforming process. Supporting structure may be fabricated and attached to electroformed pieces by conventional techniques. All materials used shall be compatible with hydrazine-type propellants, nitrogen tetroxide, water, methanol and halogenated hydrocarbon solvents.

The injector should be capable of flowing 0.12 $lbm.sec^{-1}$ of monomethyl hydrazine (per MIL-P-27404) and 0.24 $lbm.sec^{-1}$ of nitrogen tetroxide (per MSC-PPD-2A) at a pressure drop across the injector (exclusive of valves) of no greater than 40 psi. The internal injector design should be such as to allow propellants to enter the precombustion device before propellant flow from the main injection orifice begins. The total volume of the internal injector

flow passages, manifolds, and orifices should be minimized.

Boiling of the propellants within the manifolds, passageways and orifices should not occur during engine operation for periods in excess of one second. In addition, provision should be made so that the propellant valve is prevented from reaching temperatures in excess of 200°F during steady state operation or during thermal soakback.

Finally, the injector envelope and weight should be minimized.

A. Design I, Injector Face and Precombustion Cup.

In this section, the design of the injector face and precombustion cup is described. Wherever possible, critical dimensions of the Marquardt injector for the Apollo Service Module-Lunar Module RCS engine are used. The fuel flow is arbitrarily divided into three parts by mass: about 10% for precombustion and to serve as a pilot flame during combustion; about 10% for fuel film cooling of the chamber internal walls; and the remainder for the bulk flow into the combustion chamber. For minimum ignition delay time, stoichiometric proportions of the propellants should be mixed. It is recognized that during the ignition transient at startup, an infinite set of O/F ratios occur; however, it is felt that it is good design practice to proportion the propellants stoichiometrically in the precombustion cup. For monomethyl hydrazine and nitrogen tetroxide, the stoichiometric O/F is 2.5.

Precombustion Cup

The mass of fuel flowing into the precombustion cup is given by the continuity equation

$$w_f = C_D \rho_f A_f V_f \tag{1}$$

where w_f is the mass rate of fuel flow,

C_D the coefficient of discharge,

ρ_f the density,

A_f the area of the orifice, and

V_f the fuel velocity.

The fuel orifice diameter is taken as 0.0256 in. (Marquardt dimension). The fuel is considered incompressible and its density assumed 54.40 $lbm.ft^{-3}$ at $77^{o}F$. The coefficient of discharge includes a multitude of factors and relates to the ratio of actual mass flow from the orifice and the ideal mass flow. The factors encompassed therein include fluid viscosity and compressibility, flow passage geometry, velocity distribution, and vena contracta. Based on ideal conditions as a reference standard, the Marquardt injector employs a $C_D \tilde{=} 0.45$ for the fuel mass flow and a $C_D \tilde{=} 0.64$ for the oxidant mass flow. These are gross values and cannot be allocated to local parts of the injector, and are based on a pressure drop of 40 psi across the injector. These values appear rather low, especially when one considers values of $.90 \leq C_D \leq .95$ for showerhead type injectors with in line flow manifolds. Since these injectors are to be hot fired, and the performance depends in part on the miscibility of the impinging jets, then it behooves us to design the

jets so that they contain the largest kinetic energy possible. This criteria implies designing close to ideal, with the minimum flow areas for the jets. Thus, if after fabrication it is found that the flow areas are too small, then the pressure drop across the jets can be increased and a high performance injector will still result. If, instead, low C_D were assumed, and too much propellant mass flow occurred, then the pressure drop across the injector can be decreased; however, a poor performance injector would result. In view of these arguments, and recognizing that no test data is available for whole injectors fabricated by the electrodeposition process, it was decided to design close to the ideal. Thus it is assumed that 0.95 of the velocity head is converted to the kinetic energy of the fuel; therefore,

$$V_f = \sqrt{\frac{2g\Delta p.95}{\rho_f}} \tag{2}$$

where Δp is the pressure drop across the fuel orifice, i.e., 40 psi, and g is the universal gravity constant. We have

$$V_f = 80.5 \text{ ft.sec}^{-1}$$

and

$$w_f = 0.01565 \text{ lbm.sec}^{-1}.$$

This value is assumed close enough to 10% of the total fuel flow.

From Eq. (2) the oxidant velocity is calculated and it is

$$V_{ox} = 62.7 \text{ ft.sec}^{-1}$$

and the density ρ_{ox} is 89.34 lbm.ft^{-3}.

The orifice diameter is assumed 0.035 in. to give a mass flow of

$$w_{ox} = 0.0373 \text{ lbm.sec}^{-1}.$$

The calculated $^{O}/F$ is 2.38 and this value is considered close enough to the stoichiometric proportions.

The size of the precombustion cup is 0.175 in. diameter by 0.200 in. long (Fig. 1). The ignition pressure spike in the cup, which is in part a function of the cup length and diameter, cannot be ascertained at this time. The size of the cup was scaled down from previous injector designs by NASA, and by the author. One test usually made is to calculate the exit Mach number from the cup during steady state flow. The method is approximate since the stagnation pressure schedule in the cup is not known. Thus the chamber stagnation pressure is determined from

$$p^{o}_{ch} = \frac{\dot{w}\, a}{g A_t f(k)} \tag{3}$$

where a is the velocity of sound at the chamber stagnation temperature and f(k) is a function of specific heats. In this case, for the Marquardt RCS engine,

$$p^{o}_{ch} \sim 100 \text{ psia}.$$

The pressure at the cup exit is assumed the same as that of the chamber. It is assumed that about 50% of the propellant mass injected into the precombustion cup reacts; thus, the mass rate is

0.0260 lbm.sec^{-1}. The exit Mach number, M, is again determined from the mass continuity equation and is

$$w = A_{cup}\sqrt{\frac{gk\mathcal{M}}{R_o}}\ \frac{p^o_{ch}}{\sqrt{T^o_{ch}}}\ M\sqrt{1+\frac{k-1}{2}M^2} \qquad (4)$$

where M is the Mach number.

Estimated values of the stagnation temperature, T^o_{ch}, molecular weight, $\mathcal{M}$, and ratio of specific heats, k, of the combustion products are respectively: $T^o_{ch} \simeq 5280^oR$, $\mathcal{M} \simeq 22$, $k \simeq 1.2$; thus, $M_{cup} \simeq 0.9$. This value is not as ominous as it appears when one considers the concomitant pressure history in the cup. In order to achieve a Mach number of 0.9, a pressure ratio of about 0.6 is required, which increases the fictitious stagnation pressure in the cup to about 170 psia. This large pressure would cause the propellant flow into the cup to cease flowing; thus the initial assumption of 50% mass flow reaction is very conservative. At any rate, using these design values insures a large flow quantity during startup, and by aerodynamic control a diminution of the flow when it is not required as during steady state operation. A detailed "aerothermochemical" solution to this ignition transient, and also to the steady state operation of the precombustion cup is beyond the scope of this present analysis.

The design dimensions for the precombustion cup are thus maintained. One oxidant injection orifice is used, coaxial with the engine axis, with 0.035 in. diameter. Diametrically opposed fuel injection orifices are employed with 0.0180 in. diameter and slanted

downward 10^{o} so as to minimize the possibility of oxidant entrainment in the fuel passages due to unequal momentum of the fuel jets, Fig. 1C.

The design of the cooling passages for the precombustion cup was based on simply obtaining the maximum heat transfer surface and still insuring the structural integrity of the cup wall, Fig. 1D. Simple hoop stress calculations gave about 300 psi for the stresses incurred in the cup wall which is exceedingly low. No significant amelioration in heat transfer would accrue by decreasing the wall thickness since most of the thermal resistances would be contained in the fluid films adjacent to the walls.

Film Cooling Orifices

The orifice location for the fuel film cooling of the internal walls of the chamber are determined from the orifice pattern for the bulk of the propellant flow. Based on the Marquardt design, eight unlike doublets are used for the main propellant flow, Fig. 1B. One can envisage eight "plumes" of flames issuing from these doublets equally spaced peripherally in the combustor and parallel to the chamber axis. For this condition fuel film cooling on the interior walls is maximized in the region of the flame "plumes". This is accomplished by placing the fuel cooling orifices on the same radial rays as the doublets, Fig. 1B.

It was assumed that 10% of the fuel would be used for film cooling purposes. Thus the cooling fuel flow is 0.012 $lbm.sec^{-1}$.

Again assuming that .95 of the velocity head is converted to the jet kinetic energy, it is found from continuity that the fuel orifices are D_f=0.008 in. diameter. This orifice diameter is slightly less than that used by the Marquardt RCS engine. However, it is felt that it is well within good design practice and thus maintained. An angle of 30^o was used for the orifice orientation so as to get some jet spread at the impingement point and to minimize splash. This value of the impingement angle is empirical and based on the authors' discussions with other investigators and also limited observations. Since jet spread would also occur upstream, the impingement point was located 0.075 in. downstream of the injector face. With this information the location and orientation of the fuel film cooling orifices on the injector face can be determined.

Main Orifices

As stated above, the design of the orifice pattern for the bulk propellant flow is modeled from that of the Marquardt RCS engine, Fig. 1B. The orifice diameters are determined from continuity of mass flow. The location of the orifices along a radius is determined from the internal manifolds for the propellants and the following constraints: (1) maintaining the flame "plumes" as far away from the chamber internal walls as possible, and (2) orienting the doublet to obtain a concentric spray sheath (since it has been noted that radial spray patterns are sensitive to pressure disturbances and thus increase the possibility of combustion instability). The orientations of the doublet orifice passages are determined

using the Rupe criteria, and finally, the spray direction is made axial.

The doublet orifice diameters determined from the continuity equations become

$$D_{fuel} = 0.22 \text{ in. diameter}$$

$$D_{oxidant} = 0.029 \text{ in. diameter.}$$

The included angle between the fuel and oxidant orifices is assumed 60° (JPL Technical Report No. 32-255, July 15, 1965). The Rupe parameter, $\theta = \frac{(\rho V^2 d)_1}{(\rho V^2 d)_2}$ is determined and is $\theta = 0.765$.

The parameter $[\frac{1}{1+\theta}]$ is plotted versus η, which is a mixing factor. The optimum value of θ is 1; however, since the crown of the curve is flat, the value of the η-ratio for θ=0.765 is $\eta/\eta_{max} = 0.98$, and this is considered good enough. In order to orient the resultant spray coaxially, the following momentum balance equation is set up:

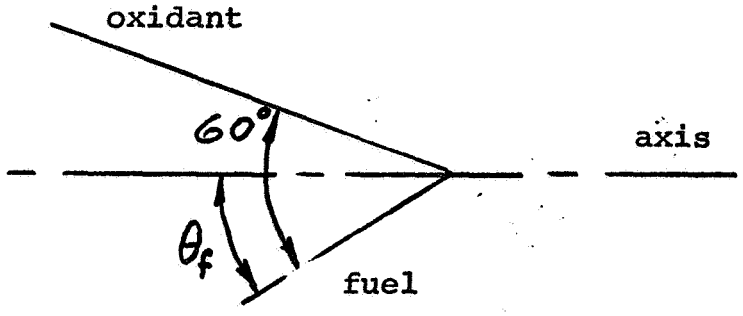

$$(wV)_f \sin\theta_f = (wV)_\theta \sin(60-\theta_f)$$

which gave

$$\theta_f = 38.6^{\circ} \text{ and } 60-\theta_f = \theta_{ox} = 21.4^{\circ}.$$

At this point all the calculable parameters for the design of the injector face are determined. The remaining design factors are compromised based on accumulated experience.

B. Design I, Internal Flow Passages.

The internal flow passages are designed with the following constraints: (1) to minimize the mass of material in the injector; (2) to minimize the occurrence of fully developed boundary layer; (3) to locate them in regions where desired heat transfer effects are obtained; (4) to allow sufficient volumes to achieve desired time delays; (5) to minimize volumes and prevent the occurrence of occluded volumes; and (6) to interface with the propellant valve such that desired feed points are obtained to the flow passages. It is seen from the above requirements that contradictions occur; thus design is based on compromise.

The fuel manifold is close to the injector face so as to cool the face. It is also close to the chamber wall, again for regenerative cooling,Fig.1D. The oxidant manifold is located farther away from the injector face to minimize the possibility of boiling during operation or soakback, Fig.1E.The center of the injector face is cooled marginally by the precombustion cup cooling annulus. The velocity of the fuel in its manifold is about 14 $ft.sec^{-1}$. The equivalent L/D for the passages,based on minimum dimensions, is about 9 which indicates that a fully developed boundary layer probably does not

occur. The fill time for the fuel manifolds, based on a step function for fuel flow from the bipropellant valve, is about 25 msec. The fuel injection delay time into the precombustion cup is about 5 msec and for the bulk flow into the combustion chamber 25 msec. The oxidant injection delay time into the precombustion cup is about 1 msec and for the bulk flow into the combustion chamber about 10 msec. From the values of delay times a starting sequence for the Marquardt RCS engine can be envisaged. Upon the bipropellant valve opening, oxidant flows into the precombustion cup. About 4 msec later, fuel flows into the precombustion cup. Due to rapid evaporation, an oxidant atmosphere builds up in the chamber and propellant mixing occurs. Based on previous analyses made by the author on engines of this size and geometry, at the end of 5 msec, full pressurization of the chamber in cold unreacted flow has not occurred. By 10 msec, full pressurization in the chamber has nearly occurred. Whether ignition occurs prior to or about this time in the precombustion cup, or whether some ignition kernels occur in the chamber is difficult to discern. By 25 msec the bulk fuel flow occurs in the chamber and the combustion process takes over.

C. Design I, Bipropellant Valve-Injector Interface.

In order to minimize the injector thickenss, two bosses are located on the aft end of the injector. Annuli are cut in these bosses to allow for "O" ring seals concentric with the propellant

ports, Fig. 1G. These ports mate with propellant ports in the exit face of the bipropellant valve. A baffle is placed between the bosses to prevent propellant mixing due to leakage and subsequent combustion.

D. Design II, Injector Face and Precombustion Cup.

The injector face for Design II is the same as that for Design I and the same criteria were used, Fig. 2A.

In Design II, a swirl cup is employed for the precombustion cup with the same mass of propellant flow into it as in Design I, Fig. 2C. Three major differences occur, namely:

(1) The propellant impact energy is not as great; thus propellant mixing in the liquid state is not as efficient. The ignition delay time may thus tend to increase where the liquid phase reaction is important. However,

(2) The propellant residence time in the precombustion cup is greater. In this case, an estimate of the residence time is calculated by following the helical path of the propellant flow in the cup, and this value is about 3 msec. Although this value is very approximate, it approaches ignition delay times for these propellants and thus allows for a greater probability that ignition occurs nearer the injector face, (thus allowing for softer starting).

(3) The third factor is that a liquid layer occurs along the internal wall of the precombustion cup, eliminating the need for internal cooling passages.

In the analysis of the pressure history in a swirl cup, a "radial" pressure gradient occurs in the propellant film thickness between the internal cup wall and the hot product gases. In some cases, the ensuing pressure drop can be significant. It is doubtful if such is the case here because the bulk propellant flow is directly into the combustion chamber rather than into the swirl cup. In other words, there will not be any significant accumulation of liquid flowing in the cup to generate large radial pressure gradients.

E. Design II, Internal Flow Passages.

In this case, the internal flow passages are particularly simple; they consist of concentric annuli, Fig. 2D,2E. Because of this simplicity, the thickness of the injector is held to a bare minimum, thus optimizing overall size or envelope and weight.

The fuel manifold is placed on the outer ring to minimize the effects of heat transfer from the chamber walls by regenerative cooling. The propellant hydrodynamics is similar to that of Design I. The fill times of the manifolds are 9 msec for the fuel and 5 msec for the oxidant. The propellant injection sequence can be envisaged to be the following: One millisecond after the propellant valve opens the oxidant flows into the swirl cup, and after two more milliseconds the fuel flows into the swirl cup. By the time the oxidant flows into the chamber, i.e., 5 msec, the contents of the swirl cup start to empty into the chamber. Pressurization begins due to evaporation, and probably due to ignition. Nine

milliseconds after the propellant valves open, the bulk fuel flows into the chamber.

F. Design II, Bipropellant Valve-Injector Interface.

The identical features occur in this case as in Design I, Fig. 2F.

III. INJECTOR FABRICATION PROCEDURE

A. Design I. (Figures 1A-1G)

1. Inspect machined mandrel.

   Position glass tubes in mandrel holes.

   Position plastic screws on circumference of mandrel.

2. Plate sufficient nickel to machine to .110 in. thickness.

   Machine per INJ 102.

   Dissolve embedded glass by immersion in hydrofluoric acid.

   Inspect and debur orifice entries.

   Remove electroform from mandrel and reposition on holder mandrel.

   Fill machined grooves with wax.

   Injection mold wax ring 1.250 in. I.D. by 1.750 in. O.D. by .100 in. thick.

   Replace .029 in. diameter glass pins in oxidizer orifices.

   Sensitize wax in machined grooves.

   Position .096 in. diameter x .375 in. long lucite rods in grooves (see INJ 106).

3. Plate .060 in. of nickel.

   Machine center of workpiece (.320 in. diameter) to a thickness of .160 in.

   Machine .016 in. slots and .175 in. diameter hole per INJ 103.

   Fill .016 in. slots with wax.

   Position pre-machined lucite plug (.175 in. diameter by .250 in. high) in .175 in. diameter hole.

4. Plate sufficient metal to machine to .200 in. thickness.

   Remove all lucite and glass pins.

   Machine per INJ 104.

   Inspect and debur all exposed orifice entries.

   Fill all exposed cavities with wax and render conductive.

   Injection mold wax ring .500 in. I.D. by .900 in. I.D. by .125 in. thick.

   Replace .096 in. diameter lucite rods.

   Position .035 in. diameter glass pin in center of .175 in. diameter wax cavity.

5. Plate sufficient nickel to machine to .300 in. thickness.

   Machine per INJ 105.

   Remove .035 in. diameter glass pin.

   Fill all exposed cavities with wax and render conductive.

   Replace .096 in. diameter lucite rods.

   Position .156 in. diameter lucite rod along axis of workpiece (see INJ 106).

6. Plate sufficient nickel to machine to .350 in. thickness.

   Machine per INJ 106.

   a. Mill semi-circular groove .125 in. wide

   Position .125 in. diameter lucite rod by .250 in. long at position of .125 in. diameter hole on INJ 106.

   Replace lucite rod in .156 in. diameter hole.

   Wax and sensitize all exposed cavities.

7. Plate sufficient metal to machine to .500 in. thickness.

   Machine per INJ 107A.

B. Design II (Figures 2A-2F)

1. Inspect machined mandrel.

   Position glass tubes in mandrel holes.

   Position plastic screws on circumference on mandrel.

2. Plate sufficient metal to machine to .090 in. thickness.

   Machine per INJ 202b.

   Dissolve embedded glass by immersion in hydrofluoric acid.

   Inspect and debur orifice entries.

   Remove electroform from mandrel and reposition on holder mandrel.

   Wax over entries to orifice.

   Press fit lucite blocks (.187 in. thick) into oxidizer and fuel manifolds.

3. Plate sufficient nickel for .165 in. machined thickness.

   Machine per INJ 203b.

   Fill .023, .031, .109, and .156 in. slots with wax. Render conductive.

Position .175 in. diameter by .250 in. long lucite plug in center hole.

Replace lucite blocks in fuel and oxidizer passages.

4. Plate sufficient nickel to machine to .200 in. thickness.

   Machine per INJ 204b.

   Fill all cavities except oxidizer manifold and .156 in. slot with wax. Render conductive.

   Position lucite blocks in oxidizer passage and .156 in. slot.

   Position .125 in. diameter lucite rod (.250 in. long) into fuel manifold (see INJ 201A for position).

5. Plate .050 in. of nickel.

   Machine per INJ 205 to .225 in. thickness.

   Remove lucite blocks from oxidizer manifold and .156 in. slot.

   Fill above cavities with wax. Render conductive.

   Reposition .125 in. diameter lucite rod.

   Position .156 in. diameter lucite rod in .156 in. slot (see INJ 201A for position).

6. Plate sufficient metal for total thickness of .400 in.

   Machine per INJ 206.

A series of working drawings which indicate the steps of the fabrication procedure are shown in Figure 1. These are for the injector with impinging jets in the precombustion cup. In Figure 2, the working drawings for the injector with tangential jets in the precombustion cup are shown. The completed injectors are shown in Figures 3 and 4, respectively.

Cleaning Procedure

1. Place injector in oven at 300°F for one-half hour to melt wax.
2. Circulate MEK through injector manifolds and orifices.
3. Repeat steps 1 and 2.
4. Clean in MEK using ultrasonic agitation (30 kc).
5. Clean in 25% hydrofluoric acid using ultrasonic agitation.
6. The units were placed in a vacuum chamber and the pressure was reduced to 1 mm. Hg.
7. Repeat steps 4 and 5.
8. Repeat step 2.

IV. TEST SPECIFICATIONS AND PROCEDURE

The injector test is comprised of three parts:

1. Flow rate versus pressure drop across injector, without propellant valve, for both fuel and oxidizer sides.
2. Percentage of total flow from each orifice in injector face.
3. High speed movies of injector processes to establish lead-lag characteristics and flow sequence.

The injector should be capable of flowing 0.12 $lbm.sec^{-1}$ of monomethyl hydrazine, (MMH), per MIL-P-27404, and 0.24 $lbm.sec^{-1}$ of nitrogen tetroxide, (NTO), per MSC-PPD-2A at a pressure difference

across injector of no greater than 40 psi. Referee fluids simulating MMH and NTO are water and trichlorethylene, respectively, (JPL 37-37, Vol. IV). The internal injector design should be such as to allow the propellant to enter the precombustion cup before propellant flow from the main orifices begins.

The basic test equipment configuration for parts 1 and 2 is shown in Figure 5. In order to adapt the injectors to the test configuration and procedure, front and back plates were designed and made, Figs. 6 and 7. In this manner, the injector can be attached to the test setup without its attendant propellant valve, and in addition, the distribution of reference fluids through the injector can be measured.

Part one consists of measuring the flow rate versus pressure drop for both fuel and oxidizer. Calibrated pressure gages were used with accuracy of one percent in the pressure gage readings with scale 0-100 psig. Graduated cylinders were used to collect the fluid flow. These were checked against reference standards. Pressure tare tests were run to compensate for pressure losses in the line between the gages and the injector entrance. Readings of the flow rate for "fuel" and "oxidizer" and the corresponding pressure differences are made. Data points include net pressure differences $30 \leq \Delta p \leq 50$ psi at 10 psi intervals. The data is corrected for density and plotted.

In Part Two of the test series, the percentage of flow through each orifice is required at design pressure difference, i.e., net Δp, Figs. 8, 9 and 10. A face plate with radially milled slots and a hole in the center was made and bolted to the injector face, Figs. 6 and 7. Holes are drilled through the face plate which connect with the milled slots. Tubing is attached to the holes and these lead to separate containers.

Duplicate runs were made with flow only in the oxidizer orifices, and this flow is ducted to the nine separate containers. The contents of the fluid in the containers is measured and the ensuing data reduced to percentages of mass distribution. A similar procedure is employed to obtain the mass distribution of fuel. Since the wall and main fuel orifices connect with the same milled slot in the face plate, the experiment is run twice. In the first run, the wall orifices are blocked by a gasket, and in the second run, the main orifices are blocked by a gasket.

Part Three of the test procedure includes taking fast motion pictures in order to determine lead-lag characteristics and flow sequence. A Hycam camera operating at 2000 pix sec^{-1} was employed, which gave a resolution time of 5×10^{-4} sec. Typical numbers range from 1 to 25 milliseconds, the former being the oxidant lag time to the injector cup, the latter the

main fuel flow lag. It is surmised that lead-lag times from 1 to 25 milliseconds can be measured with sufficient accuracy to indicate the flow sequence of the injection process.

V. RESULTS

The experimental results obtained in the three tests are presented below.

A. Calibration Runs

The reduced data of the calibration runs for both series of injector designs are shown in Figures 8 and 9. The four injectors in the Design I group are identified by the prefix I, e.g., I-1, I-2, etc.; and similarly those of Design II, e.g., II-1, II-2, etc. Water and trichlorethylene were the reference fluids for fuel and oxidant, respectively. At design point of Δp_{net}=40 psi, the data was corrected for density and the $^{O}/F$ ratio calculated for each injector. The value of the corrected $^{O}/F$ value is given to the right of the calibration curve. Nominal values of mass flow rates vs. pressure using the combined data obtained from testing all the injectors with reference fluids are given in Figure 10.

During the calibration runs, the reproducibility of collected data using a given injector was explored and it was found to be $\pm$5%, refer to Table 1. The test procedure thus was ascertained to be accurate to within $\pm$5%. This accuracy relates primarily to the error introduced by the end conditions of the particular operation in the experimental procedure. This would imply that the longer the time interval of the test operation, the more accurate the data. In practice, the time duration of the test operation was determined by the availability and size of the test apparatus.

The maximum deviation from the nominal flow curves shown in Figure 10 are: for the water mass flow rate $\pm$5%, and for the trichlorethylene $\pm$10%. If allowance is made for the accuracy inherent in the test procedure, then the deviation in the fuel mass flow falls completely within the band of test reproducibility, and the deviation in the oxidant mass flow falls within $\pm$5% of the band. It is felt that a more sophisticated analysis of the data randomness is not warranted because of the limited number of samplings available for each injector tested.

The mass flow rates are below those specified for these inejctors. Average corrected design values of oxidant and fuel flow are 0.166 and 0.077 $lbm.sec^{-1}$, with concomitant corrected $^{O}/F=2.16$. The calculated overall coefficients of discharge for the fuel and oxidant are 0.641 and 0.692, respectively. These values are based on the data averaged together for all the eight

TABLE 1

INJECTOR FLOW TEST DATA

Injector Number	Pressure Difference $lbf.ft^{-2}$	Flow H_2O, $lbm.sec^{-1}$	Flow Trichlor., $lbm.sec^{-1}$
I-1	30	.073	.146
	40	.087	.157
	50	.094	.173
I-2	20	----	.122
	30	.069	.141
	40	.087	.150
	50	.093	.162
I-3	30	.067	.147
	40	.077	.159
	50	.088	(51 psig) .179
I-4	30	.067	.144
	40	.077	.153
	50	.088	.164
II-1	25	.067	----
	30	.072	(31 psig) .150
	40	.079	(41 psig) .160
	50	.084	(51 psig) .180
II-2	30	.071	.155
	40	.082	.172
	50	.088	.183
II-3	30	.068	(31 psig) .156
	40	.081	.176
	50	.088	.192
II-4	30	.068	.156
	40	.077	.177
	50	.085	.196

Tare H_2O (without injector)	Inlet Pressure psig	Flow $lbm.sec^{-1}$
	2	.081
	5	.128
	10	.171
	15	.202
	20	.236

TABLE 1 (Continued)

Tare Trichlor. (without injector)	Inlet Pressure psig	Flow $lbm.sec^{-1}$
	6	.201
	11	.282
	15	.371

Test medium: H_2O, trichlorethylene

Test temperature: Room ambient, $75^{o}F \pm 10^{o}F$

injectors. The calculated coefficients of discharge for the Marquardt injector are 0.45 and 0.64 for fuel and oxidant, respectively. It is seen that the use of these values of C_D for the design of the Camin injectors would have produced significant deviations in the fuel flow rates. Corrections to the mass flow rates could have been achieved by lowering the pressure drop across the injector. However, during a hot firing, the probable performance of the injector would be low due to poor propellant mixing. Thus, by increasing the pressure drop across the Camin injectors to 96.8 psi and 83.6 psi for the fuel and oxidant, respectively, the design mass flow of the propellants can be achieved, with concomitant good mixing and probable good performance.

The design $^O/F$ ratio is 2.00; that obtained from the nominal test values is 2.16. If allowance is made for the accuracy in the test procedure, then the spread in $^O/F$ is $1.85 \leq {}^O/F \leq 2.50$. The spread in the calculated $^O/F$ ratios based on the measured values of mass flow is $1.88 \leq {}^O/F \leq 2.45$. It is thus seen that the experimental deviation in the $^O/F$ ratio is less than that predicted by the error analysis based on the nominal propellant flow rates.

B. Propellant Flow Distribution

The total flow from each orifice is shown in Table 2, and the reduced data in Table 3. The mass flow times for the cooling and main orifices are 30 sec and 5 sec, respectively. The design values

TABLE 2

INJECTOR FLOW TEST DATA

TOTAL FLOW FROM EACH ORIFICE

(cc) CUBIC CENTIMETER

Specimen		Cup	1	2	3	4	5	6	7	8
I-1	Cooling Orifice		14	7	11	14.5	19.5	16	17	16.5
	Fuel Orifice	35	29	26	30.5	29	28	32	27.5	32
	Oxidant Orifice	37	32	33	33	33	30	33	32	34
I-2	Cooling Orifice		16	16	16	2.4	17	17	17	5
	Fuel Orifice	28	22.5	24	24	38	22	26	23	32
	Oxidant Orifice	23	42	39	39	36	36	40	37	38.5
I-3	Cooling Orifice		17	17	17.5	18	22	18	17	16
	Fuel Orifice	46	36	35	30	34	33	32	31	35
	Oxidant Orifice	52	35	37	32	34	36	34	34	34
I-4	Cooling Orifice		16.5	19	28	17	16	16	20	16
	Fuel Orifice	20	18.5	22	22	19.5	19	22	24	9
	Oxidant Orifice	61	29	36	27	28	26	30	26	30
II-1	Cooling Orifice		24	20	21	19	24	19	18.5	12
	Fuel Orifice	5	19.5	19.5	21	20	21	19	21	20
	Oxidant Orifice	33.0	28.5	28.5	31	30	30	31.5	30	32

TABLE 2 (Contd.)

Specimen		Cup	1	2	3	4	5	6	7	8
II-2	Cooling Orifice		17	20	2.5	17	17.5	32.5	17.5	17.0
	Fuel Orifice	20	24	23.5	21	24	25	49	25	24
	Oxidant Orifice	40	36	35	37	39	38	37	35	37
II-3	Cooling Orifice		18.5	16	.6	17	4.9	19.5	19.0	17.5
	Fuel Orifice	34	28	26.5	28.5	26	28	26	27	31
	Oxidant Orifice	49	34	35.5	34.5	34.5	36.5	36.5	37.0	34.5
II-4	Cooling Orifice		17.5	16.5	4.5	16.5	10	17.5	18	16.5
	Fuel Orifice	30	27	26	27	26.5	26	28	27.5	27
	Oxidant Orifice	46.5	32	35.5	34.5	34.5	35.5	36	36.5	35

TABLE 3

PROPELLANT DISTRIBUTION IN INJECTORS

Specimen	Total Fuel Flow cc H_2O	Total Oxidant Flow cc Trichlorethylene	% Fuel Flow in Cup	% Oxidant Flow in Cup	% Fuel Flow for Cooling	Corrected (O/F) Cup	Overall O/F	O/F Calibration Data
I-1	287.9	297.0	12.1	12.4	6.6	1.6	1.59	2.00
I-2	247.3	320.5	11.3	7.2	7.2	1.9	2.00	1.92
I-3	335.4	338.0	13.7	15.4	7.0	1.8	2.05	2.16
I-4	201.1	293.0	10.0	20.8	12.5	4.7	2.25	1.88
II-1	192.3	274.5	2.3	12.0	13.7	10.2	2.20	2.17
II-2	239.0	334.0	8.4	12.0	9.9	3.1	2.16	2.28
II-3	273.8	332.0	12.4	14.7	6.9	2.3	2.86	2.35
II-4	263.5	326.0	11.4	16.1	7.0	2.3	1.98	2.45

used for the propellant flow into the cup are: 13.0% and 15.5% fuel and oxidant mass flow, respectively, with an $^{O}/F=2.38$. It is seen that with the exception of injector II-1 where the fuel orifice is obviously clogged, the flow values are in the ball park; namely, the average values are 12.7% and 14.1% for fuel and oxidant, respectively. If we consider the percentage difference in flow values based on design values, then the fuel flow deviation is $-4.6\% \leq \Delta\dot{m}_f \leq 0.7\%$ and the oxidant flow $-8.5\% \leq \Delta\dot{m}_o \leq 5.3\%$. It is seen that flow deficiencies are more prevalent. A check of the cleaning procedure is indicated.

The design percentage of fuel flow for film cooling was 10%. The average experimental value was 8.9% with a deviation in percentage flow based on design values of $-3.4\% \leq \Delta\dot{m}_f \leq 3.7\%$. A cursory view of the data in Table 2 for the flow through the main fuel and oxidant orifices indicates that only five out of 128 orifices show a significant deviation in flow. These are given below in terms of volume flow deviation, Δv, from the mean flow, $\bar{v}$,

Specimen II-2 $\Delta v_f = +25$ cc , $\bar{v}_f = 24$ cc

I-2 $\Delta v_f = +14$ cc , $\bar{v}_f = 24$ cc

$\Delta v_f = +\ 8$ cc , $\bar{v}_f = 24$ cc

I-4 $\Delta v_f = -12$ cc , $\bar{v}_f = 21$ cc

$\Delta v_o = +\ 8$ cc , $\bar{v}_o = 28$ cc

The number of orifices for film cooling which indicate a flow deviation are more numerous, namely, 11 out of 64. In all cases except two, however, the mass of fuel flow is less than the orifice mean flow, which implies that some sort of blockage exists in the orifices. Again the cleaning procedure is suspect and more effort will be expended in this area.

A photograph of the injector I-2 flowing at design Δp=40 psi is given in Figure 11. It is seen that the bulk flow is parallel and normal to the injector plate.

C. Injector Time Lead and Lag

Lead and lag times for the injector-valve combination were determined by means of high speed photography at 2000 frames per second. Lead-lag times for the injector valve were calculated and it was found that the time interval between the electric pulse to open the valve and the appearance of the fuel flow was .053 sec. The oxidant jet then appeared lagging the fuel by .002 sec, Figure 12.

Table 4 presents the propellant lag times. It is noted that in this study all time lags are referenced to the appearance of propellant flow from the precombustion cup. This proved necessary since it was not possible to obtain and record a signal from the propellant valve actuation circuit. The values given are corrected

TABLE 4

INJECTOR LAG TIMES USING CUP FLOW AS ZERO REFERENCE

Injector Valve Opening - Fuel Flow Lag - .053 sec
- Oxidant Flow Lag - .002 sec

Specimen	Cup Flow Time, sec	Corrected Oxidant Flow Lag, sec	Corrected Fuel Flow Lag sec
I-1	0	.006	.058
I-2	0	.002	.053
I-3	0	.006	.053
I-4	0	.005	.066
II-1	0	0	.009
II-2	0	0	.011
II-3	0	0	.013
II-4	0	0	.011

for the fuel lead in the propellant valve. Injector specimen series I-1 - I-4 contains the impinging jets in the cup and specimen series II-1 - II-4 contains the swirl cup. The performance of series II-4 indicates that there is no discernible time lag between cup flow and oxidant flow. This value agrees with that predicted in the design study (refer to Interim Report, March 1968). The fuel lag is about .011 sec., and this value agrees well with the theoretically predicted value of .009 sec. These values agree very well. However, it was noted in the previous calibration runs that a typical cone spray geometry from the swirl cup was not observed.

The performance of the injector specimen series I-1 to I-4 gives an average oxidant lag time of about .005 sec, including specimen I-2 which deviates somewhat with a value of .002 sec. The predicted delay time as determined from time values given in the aforementioned interim report is .007 sec. The average measured fuel lag time is .056 sec with -.003 to .010 sec deviations. This value compares with the predicted value of .025 sec. In this case it is seen that the oxidant delay agrees well; however, the fuel delay is about twice that estimated. One reason that can explain the deviation in the fuel lag time is that it was calculated assuming a step function in the fuel flow. Reference

to Figure 12 shows that the fuel flow geometry differs significantly from a step function. In addition, the fuel flow passages in injectors I-1- I-4 contain several abrupt turns in which the flow is stagnated, which decreases the mean flow velocity. Thus the value of the flow velocity used to calculate the fuel lag time may have been optimistic.

VI. CONCLUSIONS

A program was conducted to demonstrate the feasibility of fabricating injectors by the electroforming process. The scope of this program consisted of designing, fabricating and hydraulically flow testing 100-pound thrust rocket engine injectors for use with hypergolic earth storable bipropellants.

Six conceptual injector designs were generated, of which two were selected for fabrication. Four injectors of each configuration were fabricated and subjected to testing in order to demonstrate reproducibility of design and hydraulic characteristics.

The results of this investigation indicate that injectors can be fabricated by the electroformation process. The injectors can include intricate internal flow geometry and can be free of welds, interference fits, brazed joints. Reproducibility of dimension and hydraulic characteristics is as good as the state-of-the-art injectors manufactured by conventional machining methods.

Additional effort is required in the cleaning process for small diameter holes in order to better their hydraulic characteristics.

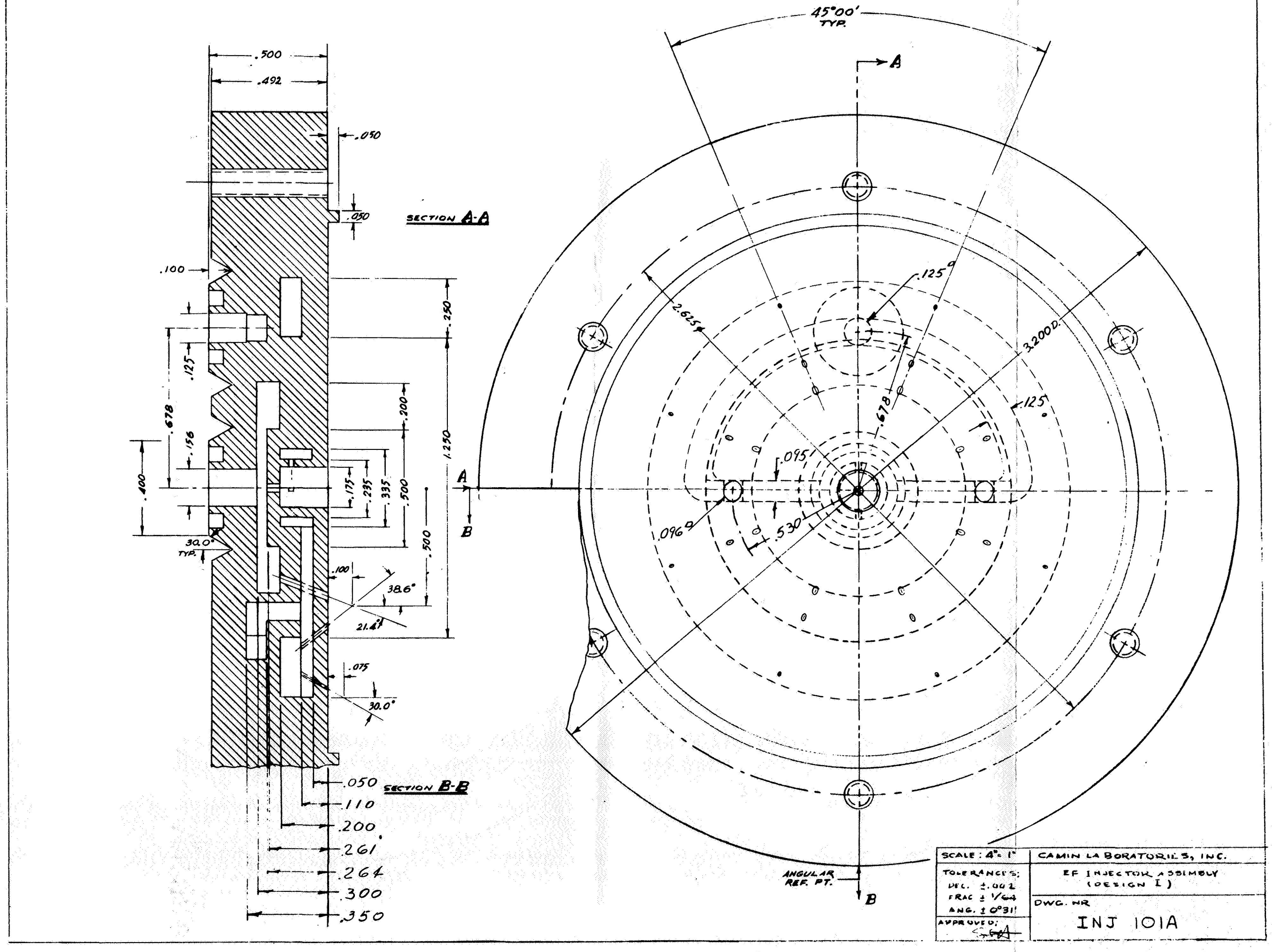

FIG. 1A. WORKING DRAWING FOR 100-POUND THRUST INJECTOR WITH IMPINGING JETS IN PRECOMBUSTION CUP, DESIGN I

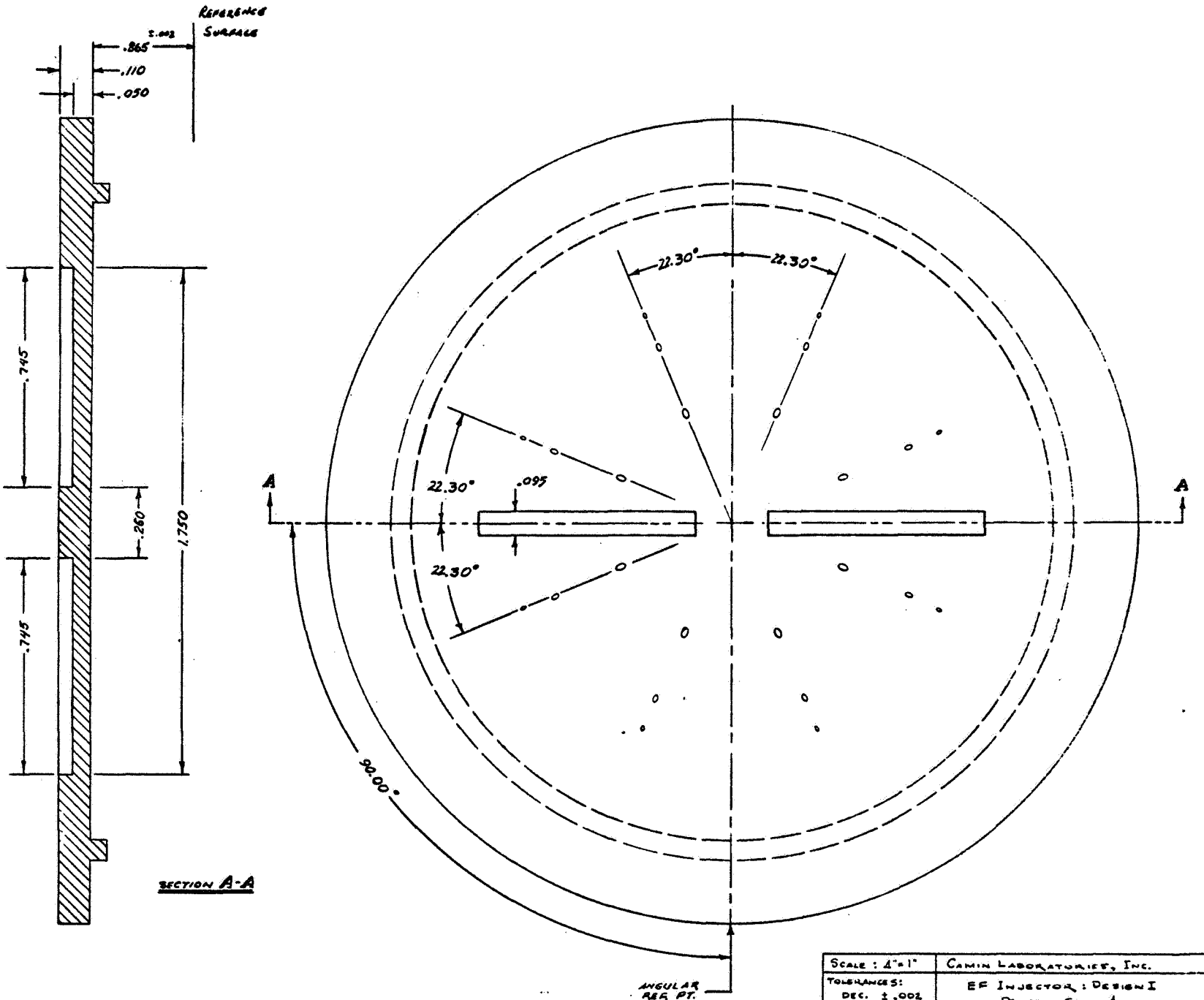

FIG. 1B. WORKING DRAWING FOR 100-POUND THRUST INJECTOR WITH IMPINGING JETS IN PRE-COMBUSTION CUP, DESIGN I

SCALE : 4"=1"	CAMIN LABORATORIES, INC.
TOLERANCES: DEC. ± .002 FRAC. ± 1/64 ANG. ± 0°31'	EF INJECTOR : DESIGN I PROCESS STEP 1
APPROVED:	DWG. NR. INJ-102

NOTE: DO NOT FACE OFF ENTIRE BAFFLE SURFACE
FACE OFF ONLY .320 DIA AREA IN CENTER.

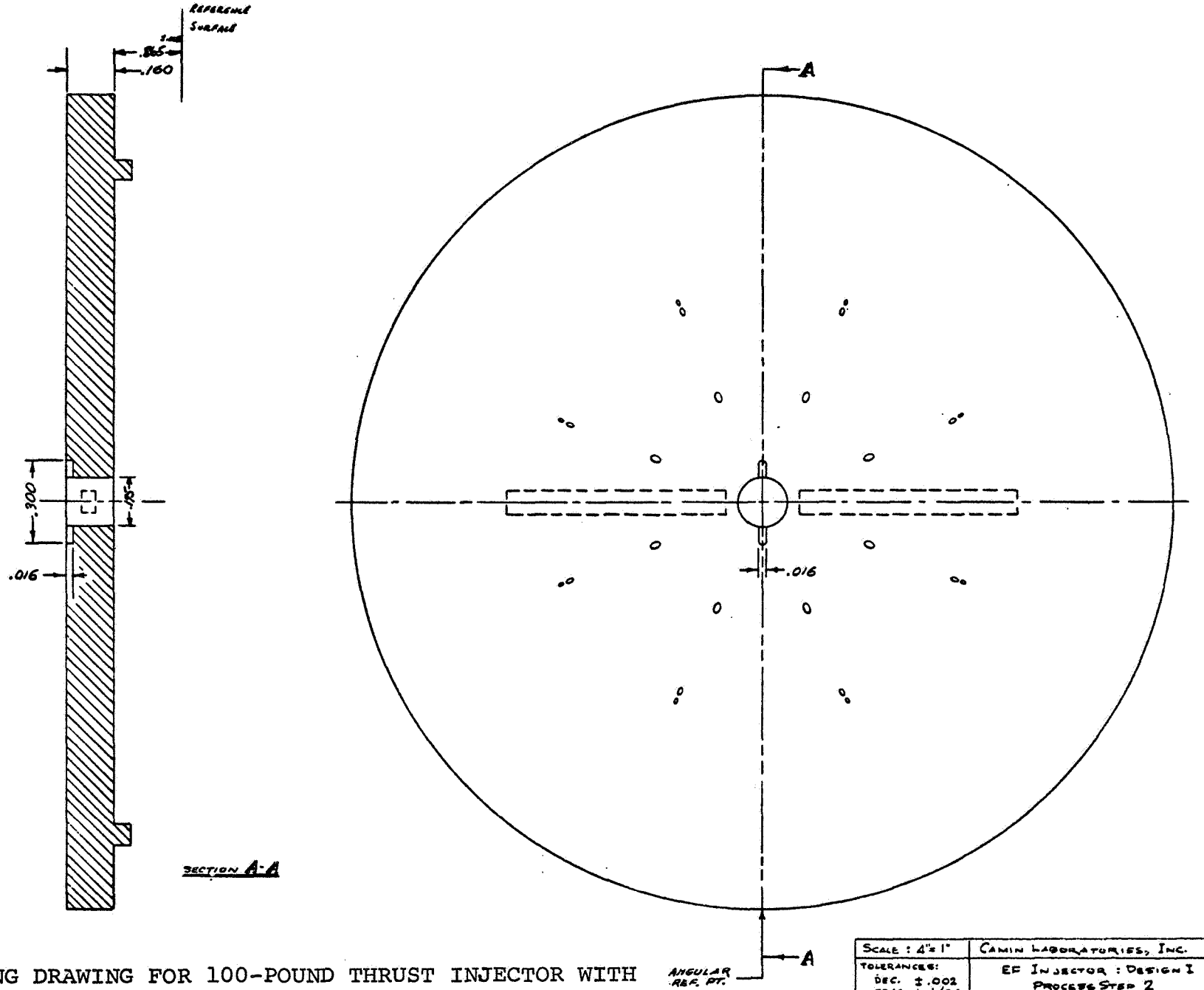

FIG. 1C. WORKING DRAWING FOR 100-POUND THRUST INJECTOR WITH IMPINGING JETS IN PRE-COMBUSTION CUP, DESIGN I

SCALE : 4" = 1"	CAMIN LABORATORIES, INC.
TOLERANCES: DEC. ± .002 FRAC. ± 1/64 ANG. ± 0°31'	EP INJECTOR : DESIGN I PROCESS STEP 2
APPROVED: SRA	DWG. NO. INJ 103

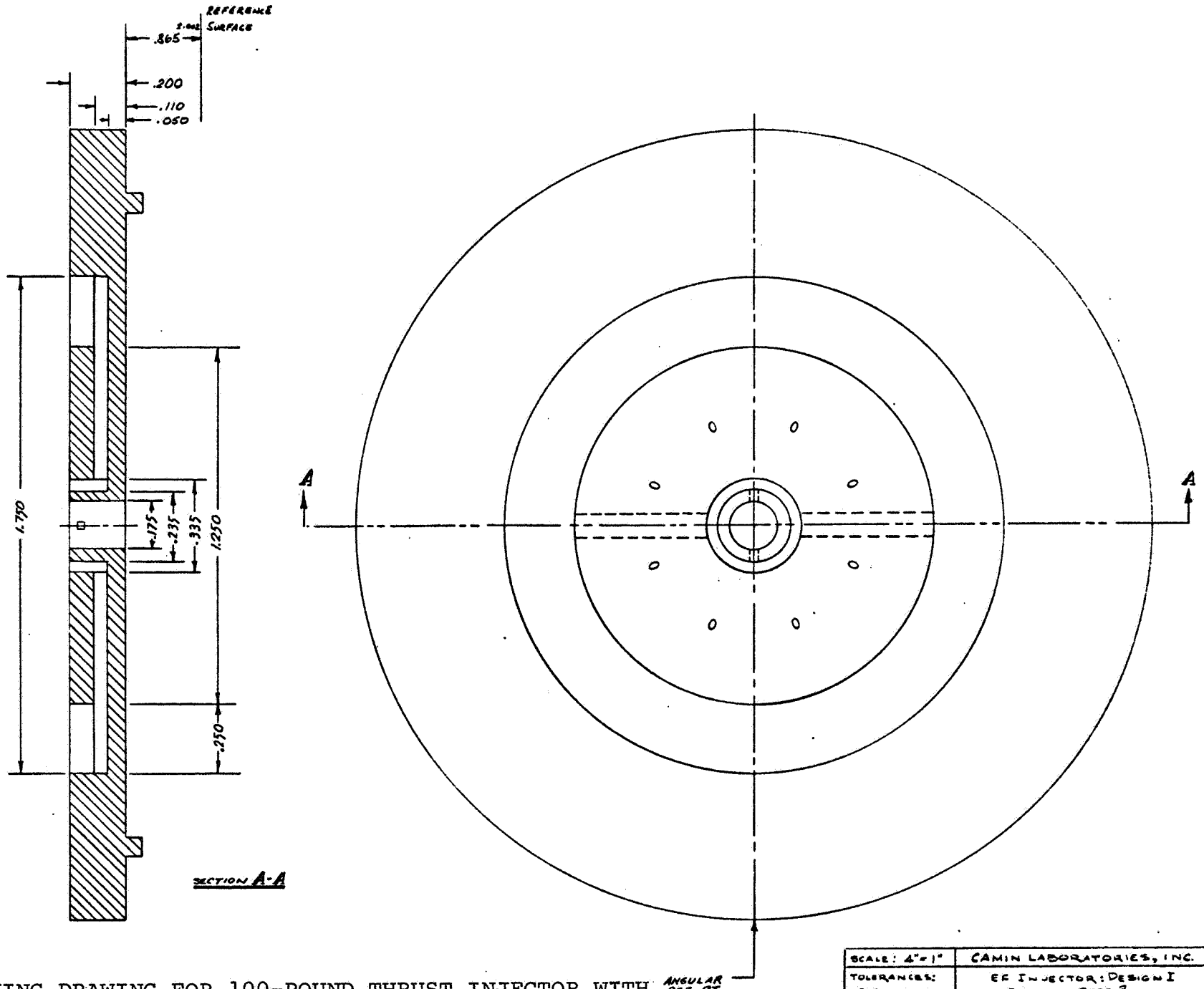

SCALE: 4"=1"	CAMIN LABORATORIES, INC.
TOLERANCES: DEC. ±.002 FRAC. ± 1/64 ANG. ± 0°31'	EF INJECTOR: DESIGN I PROCESS STEP 3
APPROVED:	DWG. NR. INJ 104

FIG. 1D. WORKING DRAWING FOR 100-POUND THRUST INJECTOR WITH IMPINGING JETS IN PRE-COMBUSTION CUP, DESIGN I

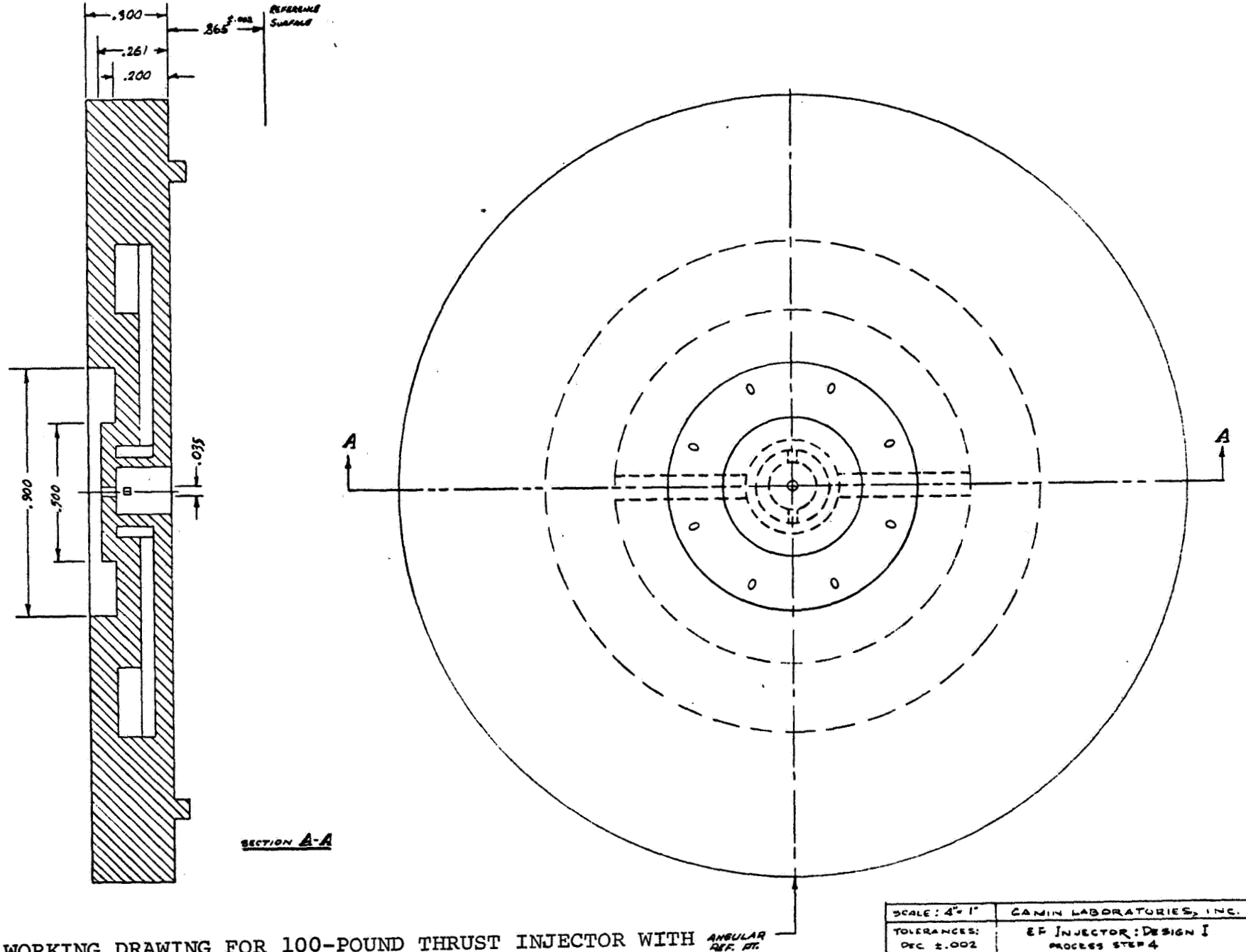

SCALE: 4" = 1"	CAMIN LABORATORIES, INC.
TOLERANCES: DEC. ±.002 FRAC. ± 1/64 ANG. ± 0° 31'	EF INJECTOR: DESIGN I PROCESS STEP 4
APPROVED:	DWG. NR. INJ 105

FIG. 1E. WORKING DRAWING FOR 100-POUND THRUST INJECTOR WITH IMPINGING JETS IN PRE-COMBUSTION CUP, DESIGN I

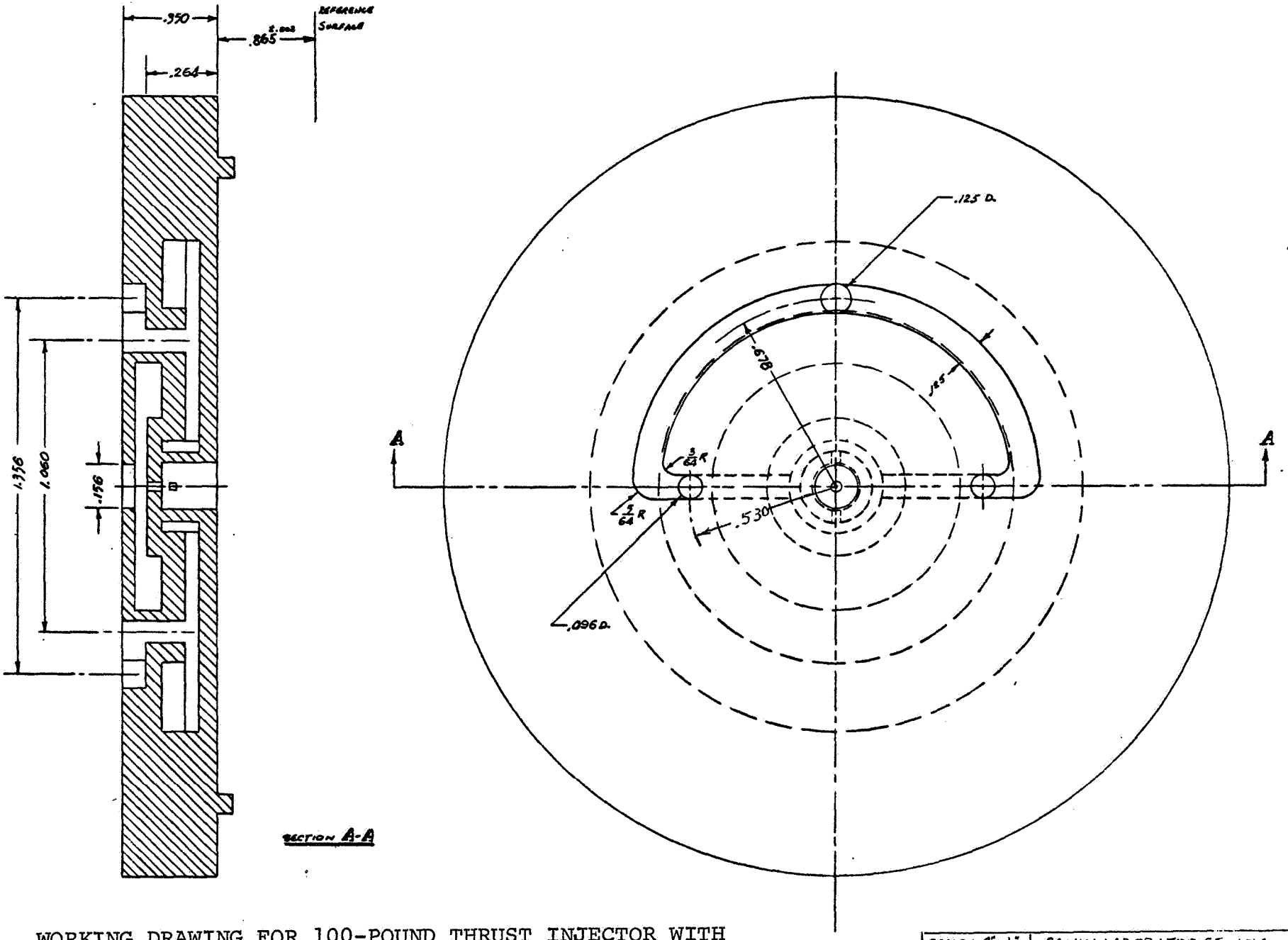

FIG. 1F. WORKING DRAWING FOR 100-POUND THRUST INJECTOR WITH IMPINGING JETS IN PRE-COMBUSTION CUP, DESIGN I

SCALE: 4"=1"	CAMIN LABORATORIES, INC.
TOLERANCES: DEC. ±.002 FRAC. ± 1/64 ANG. ± 0°31'	EF INJECTOR: DESIGN I PROCESS STEP 5
APPROVED:	DWG. NR. INJ 106

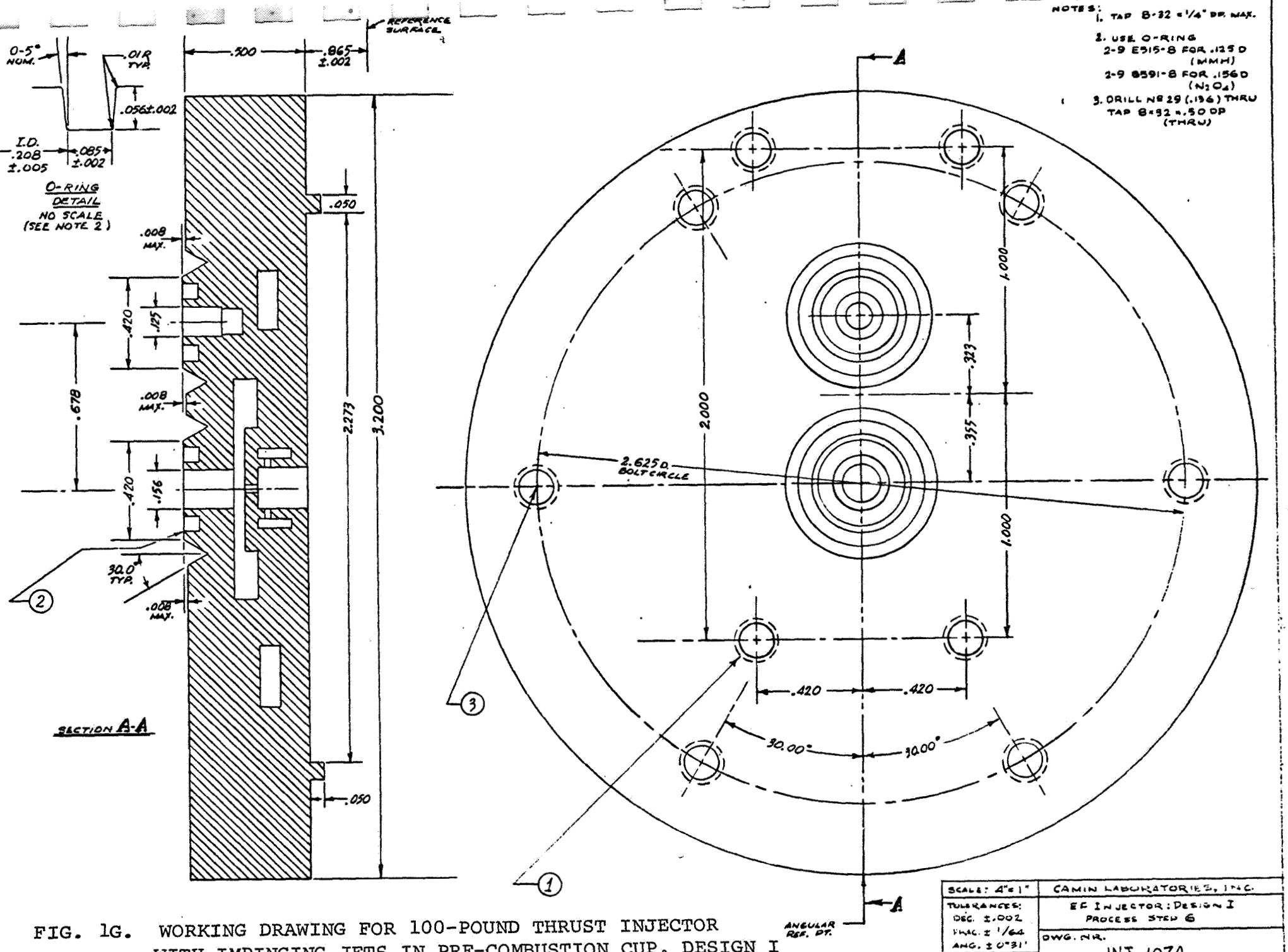

FIG. 1G. WORKING DRAWING FOR 100-POUND THRUST INJECTOR WITH IMPINGING JETS IN PRE-COMBUSTION CUP, DESIGN I

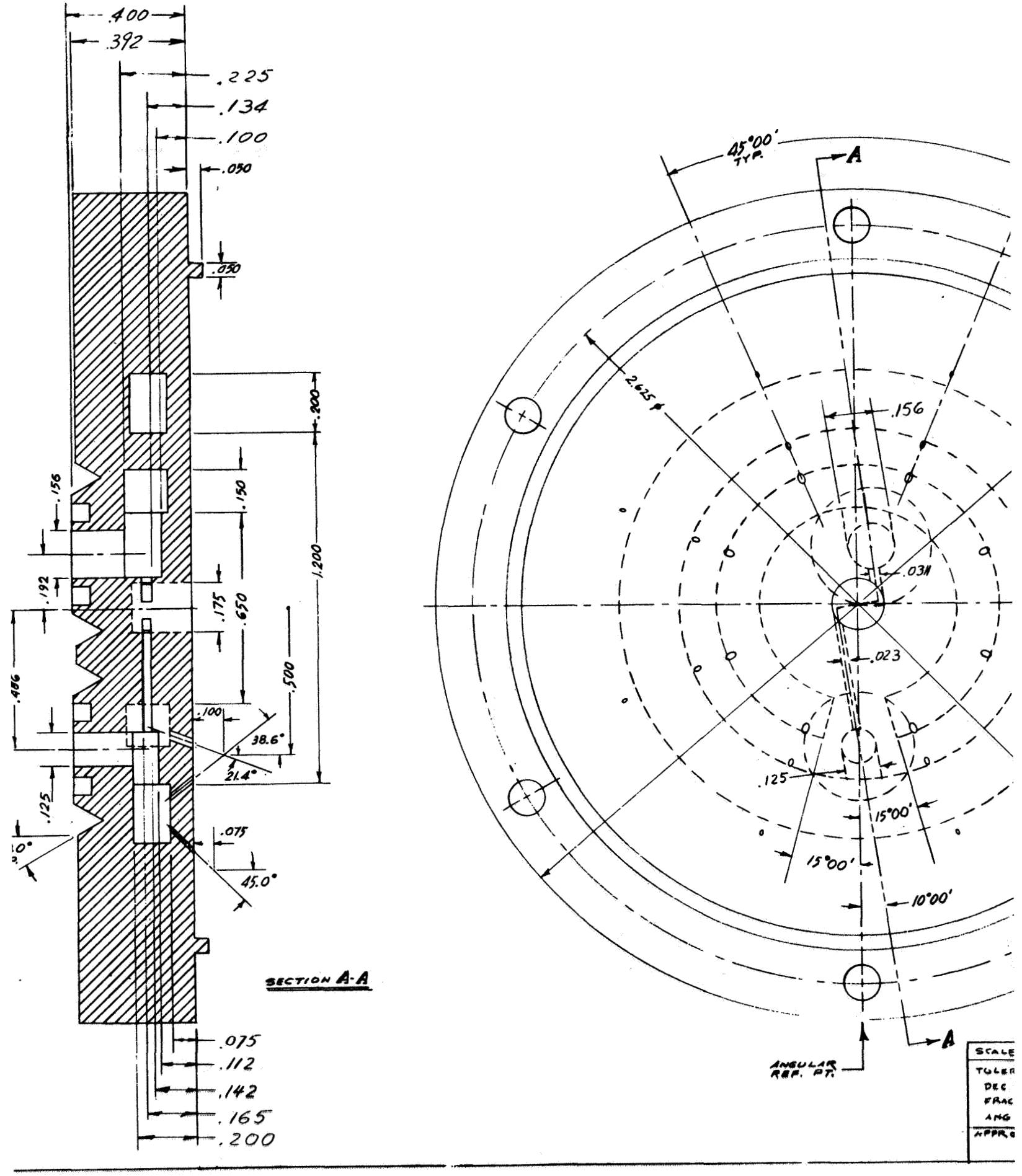

FIG. 2A. WORKING DRAWING FOR 100-POUND THRUST INJECTOR WITH TANGENTIAL JETS IN PR

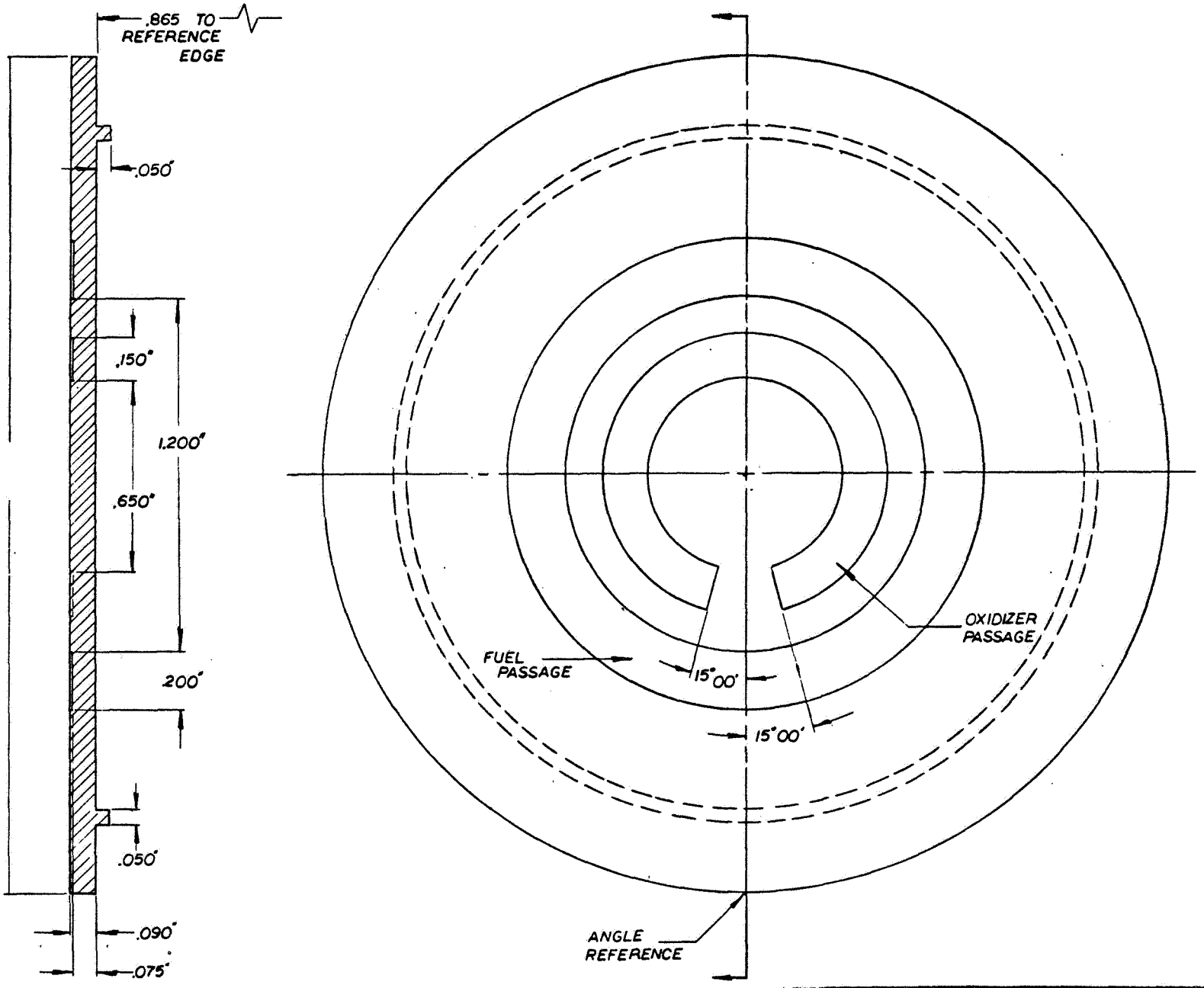

FIG. 2B. WORKING DRAWING FOR 100-POUND THRUST INJECTOR WITH TANGENTIAL JETS IN PRE-COMBUSTION CUP, DESIGN II

DRAWN 5-31-68 MWD	CAMIN LABORATORIES
APP'D:	BROOKLYN, NEW YORK
SCALE: 4X	TITLE: E.F. INJECTOR
TOLERANCES UNLESS NOTED NON-ACCUMULATIVE	DESIGN II DWG 1
FRACTIONS ± 1/64"	DWG. NO. EFM INJ 202b
DECIMALS ± .002"	
ANGULAR ± 0°31'	

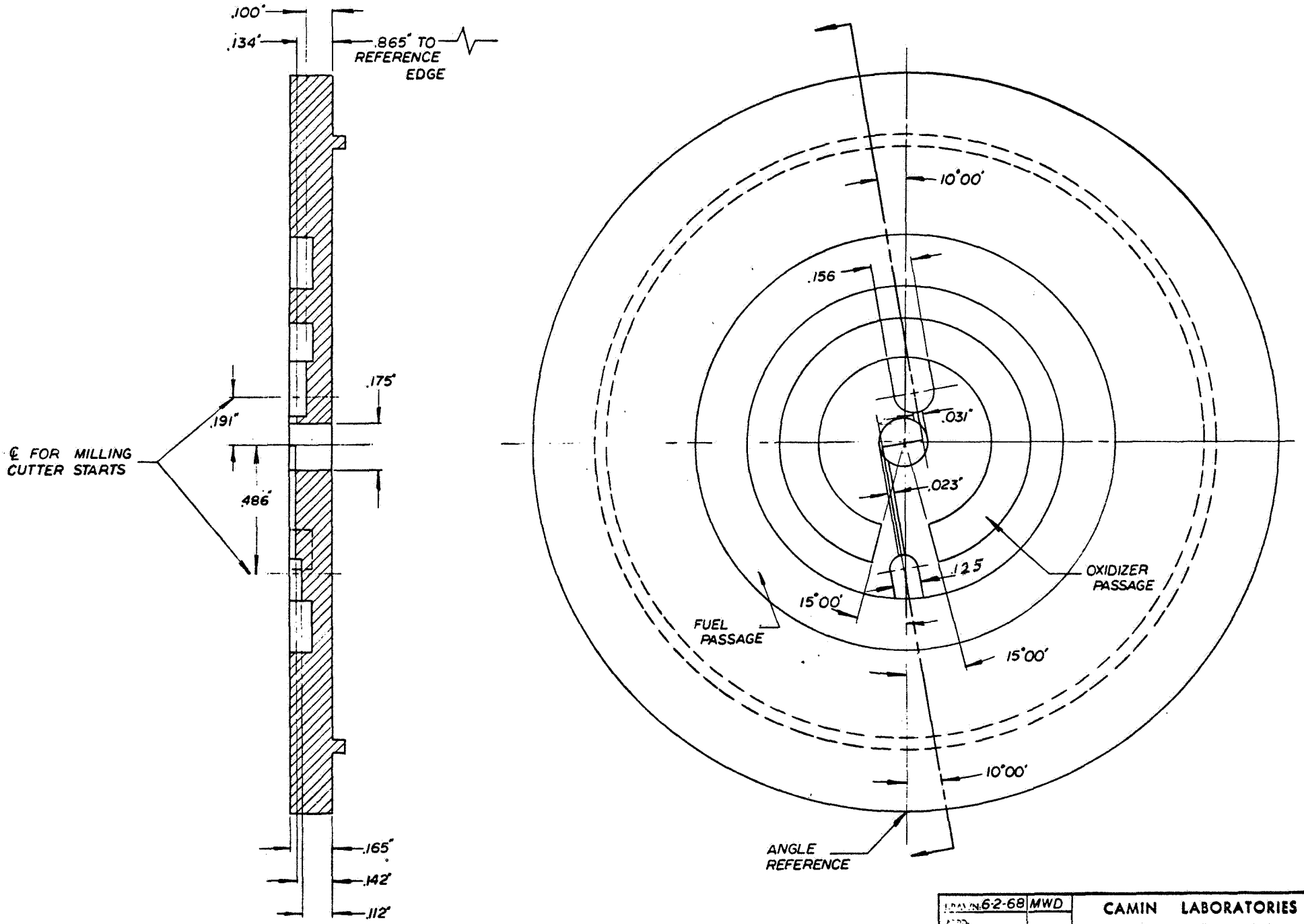

FIG. 2C. WORKING DRAWING FOR 100-POUND THRUST INJECTOR WITH TANGENTIAL JETS IN PRE-COMBUSTION CUP, DESIGN II

DRAWN 6-2-68 MWD	CAMIN LABORATORIES
APPD.	BROOKLYN, NEW YORK
SCALE 4X	TITLE: E F INJECTOR
TOLERANCES UNLESS NOTED NON-ACCUMULATIVE	DESIGN II DWG. 2
FRACTIONS ± 1/64"	DWG. NO. EFM INJ 203b
DECIMALS ± .002"	
ANGULAR ± 0°31'	

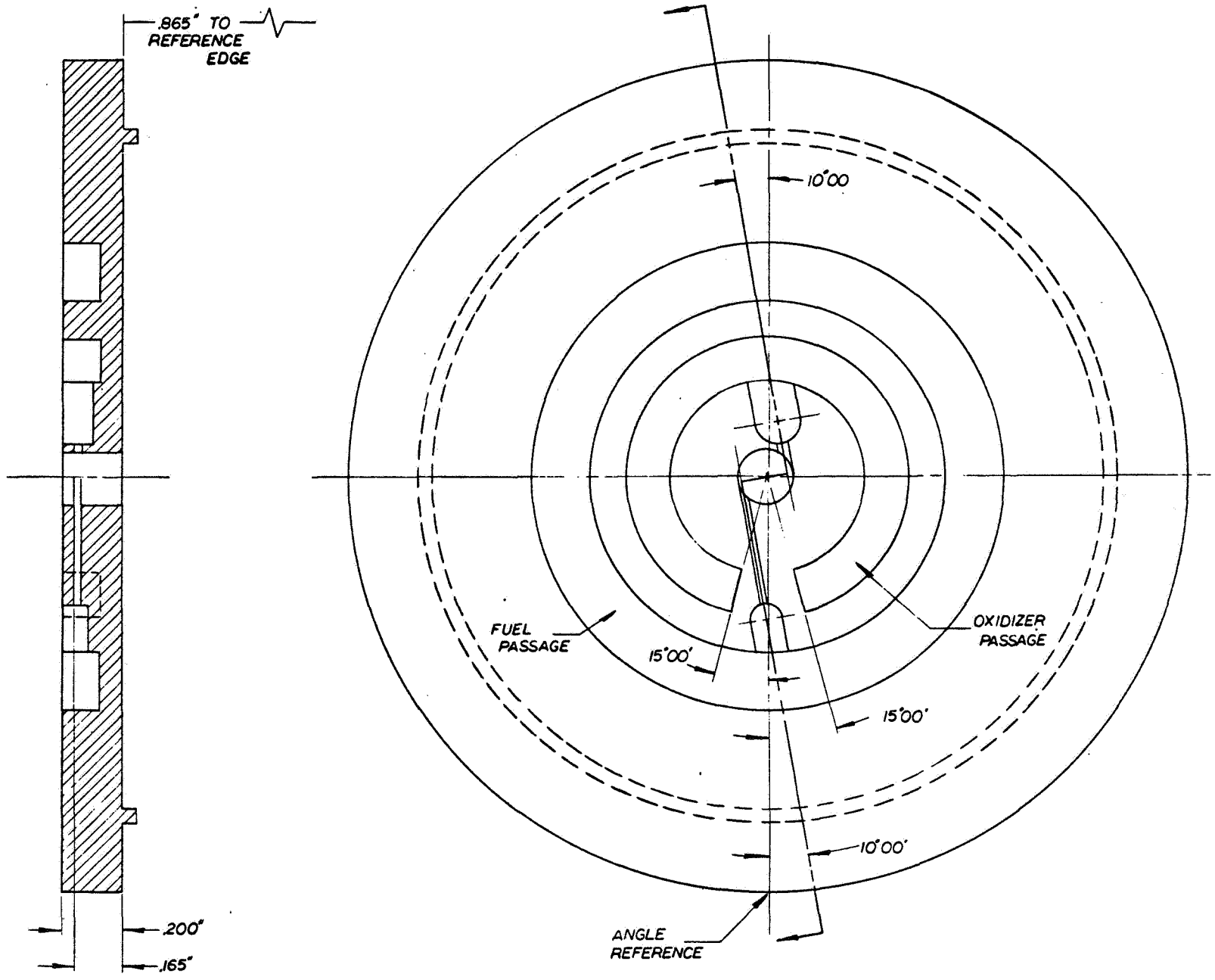

FIG. 2D. WORKING DRAWING FOR 100-POUND THRUST INJECTOR WITH TANGENTIAL JETS IN PRE-COMBUSTION CUP, DESIGN II

DRAWN 6-5-68 MWD	CAMIN LABORATORIES
APPD:	BROOKLYN, NEW YORK
SCALE: 4X	TITLE: E.F. INJECTOR
TOLERANCES UNLESS NOTED NON ACCUMULATIVE	DESIGN II DWG 3
FRACTIONS ± 1/64"	DWG. NO. EFM-INJ-204b
DECIMALS ± .002"	
ANGULAR ± 0°31'	

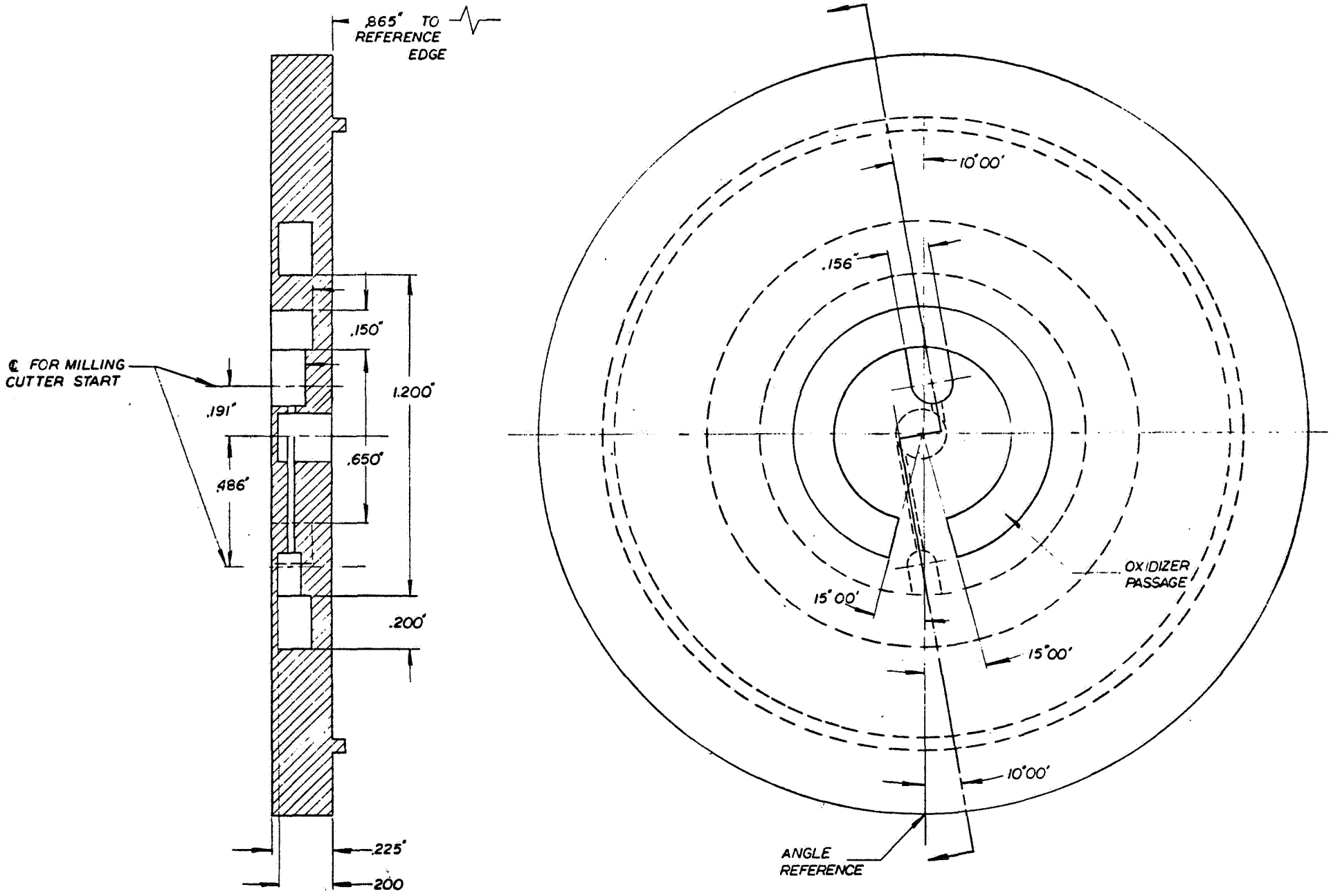

FIG. 2E. WORKING DRAWING FOR 100-POUND THRUST INJECTOR WITH TANGENTIAL JETS IN PRE-COMBUSTION CUP, DESIGN II

DRAWN 6-3-68 MWD		CAMIN LABORATORIES
APPD.		BROOKLYN, NEW YORK
SCALE 4X	TITLE:	EF INJECTOR
TOLERANCES UNLESS NOTED NON-ACCUMULATIVE		DESIGN II DWG 4
FRACTIONS ± 1/64"	DWG. NO.	EFM-INJ-205
DECIMALS ± .002"		
ANGULAR ± 0°31'		

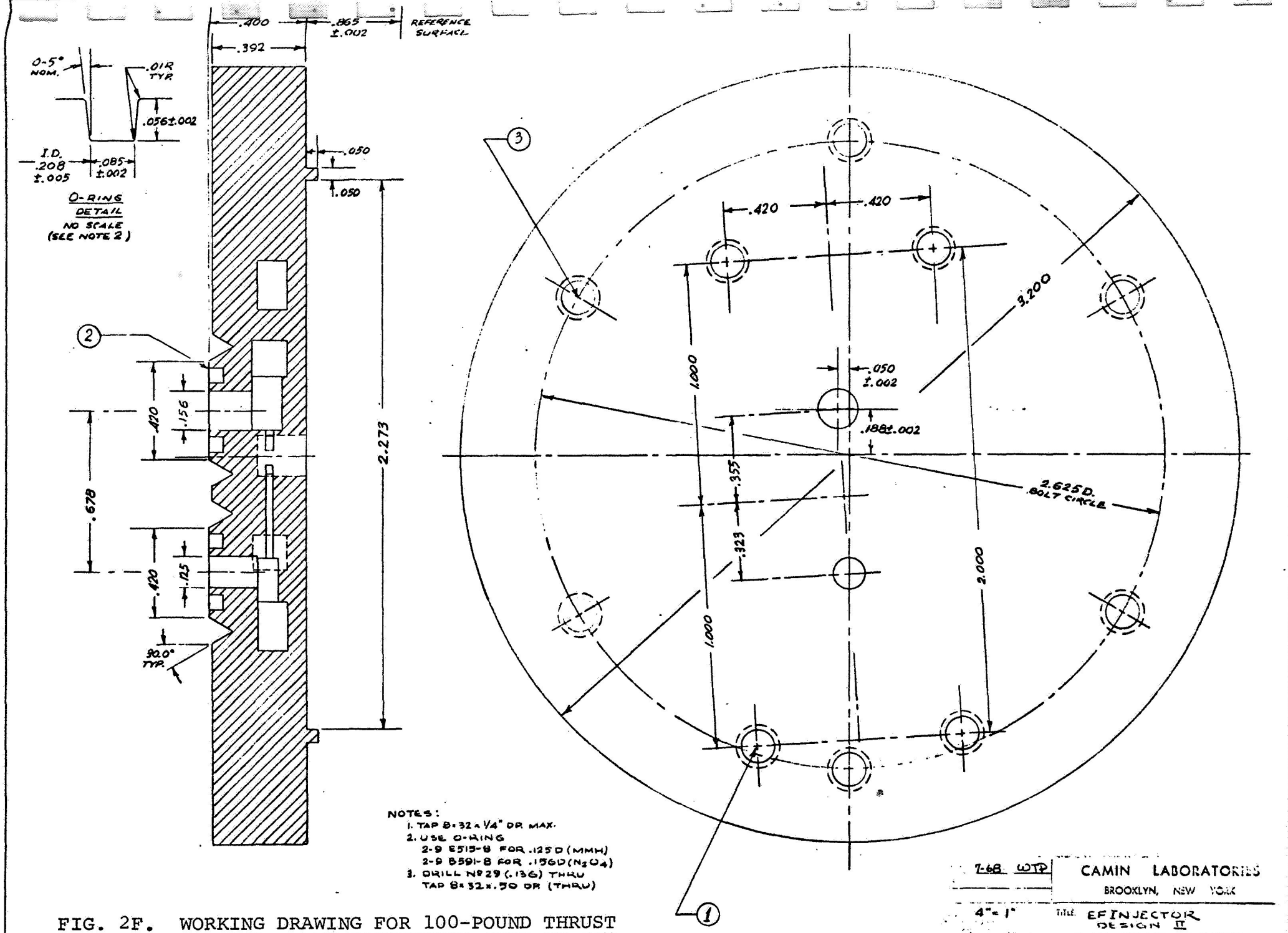

NOTES:
1. TAP 8-32 x 1/4" DP MAX.
2. USE O-RING
   2-9 E515-8 FOR .125D (MMH)
   2-9 B591-8 FOR .156D (N_2O_4)
3. DRILL №29 (.136) THRU
   TAP 8-32 x .50 DP (THRU)

7-68 WTP	CAMIN LABORATORIES	
	BROOKLYN, NEW YORK	
4"=1"	TITLE: EF INJECTOR DESIGN II	
1/64	FINAL PROCESS STEP	
DECIMALS = .005	DWG. NO.	INJ 206
ANGULAR = 0°30'		

FIG. 2F. WORKING DRAWING FOR 100-POUND THRUST INJECTOR WITH TANGENTIAL JETS IN PRE-COMBUSTION CUP, DESIGN II

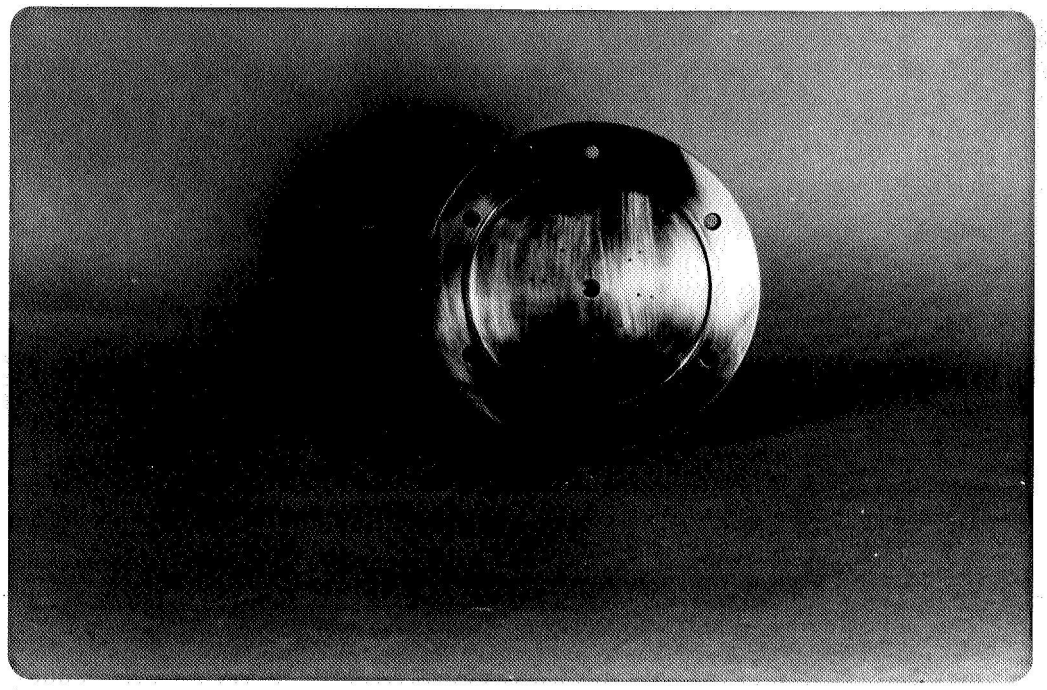

FIGURE 3. FACE PHOTOGRAPH OF 100-POUND THRUST INJECTOR WITH PRECOMBUSTION CUP, IMPINGING JETS IN PRECOMBUSTION CUP

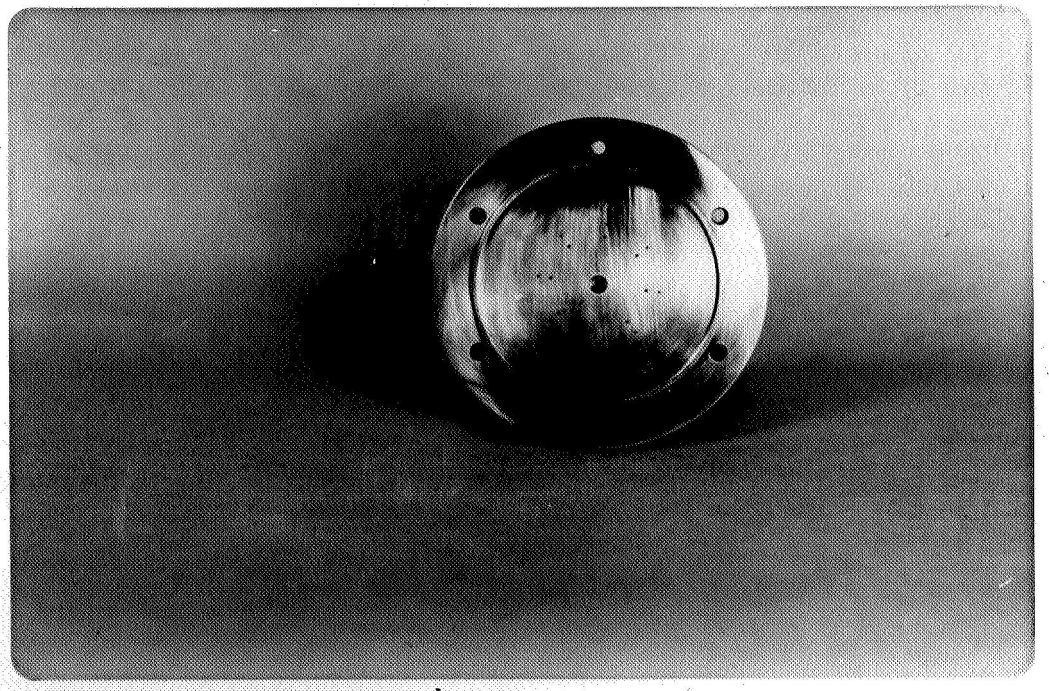

FIGURE 4. FACE PHOTOGRAPH OF 100-POUND THRUST INJECTOR WITH PRECOMBUSTION CUP, TANGENTIAL JETS IN PRECOMBUSTION CUP

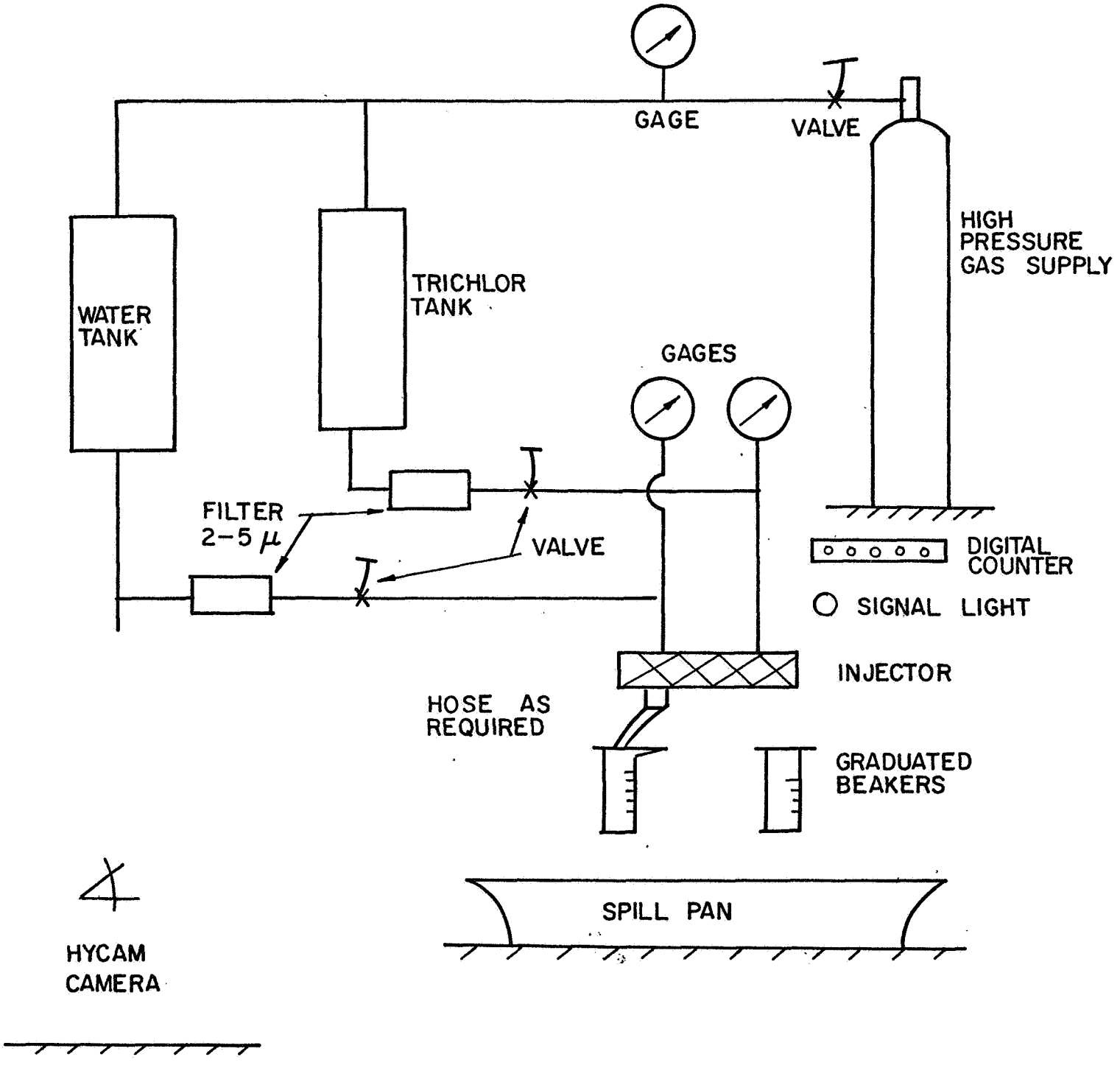

FIG. 5A. TEST CONFIGURATION AND PHOTOGRAPH

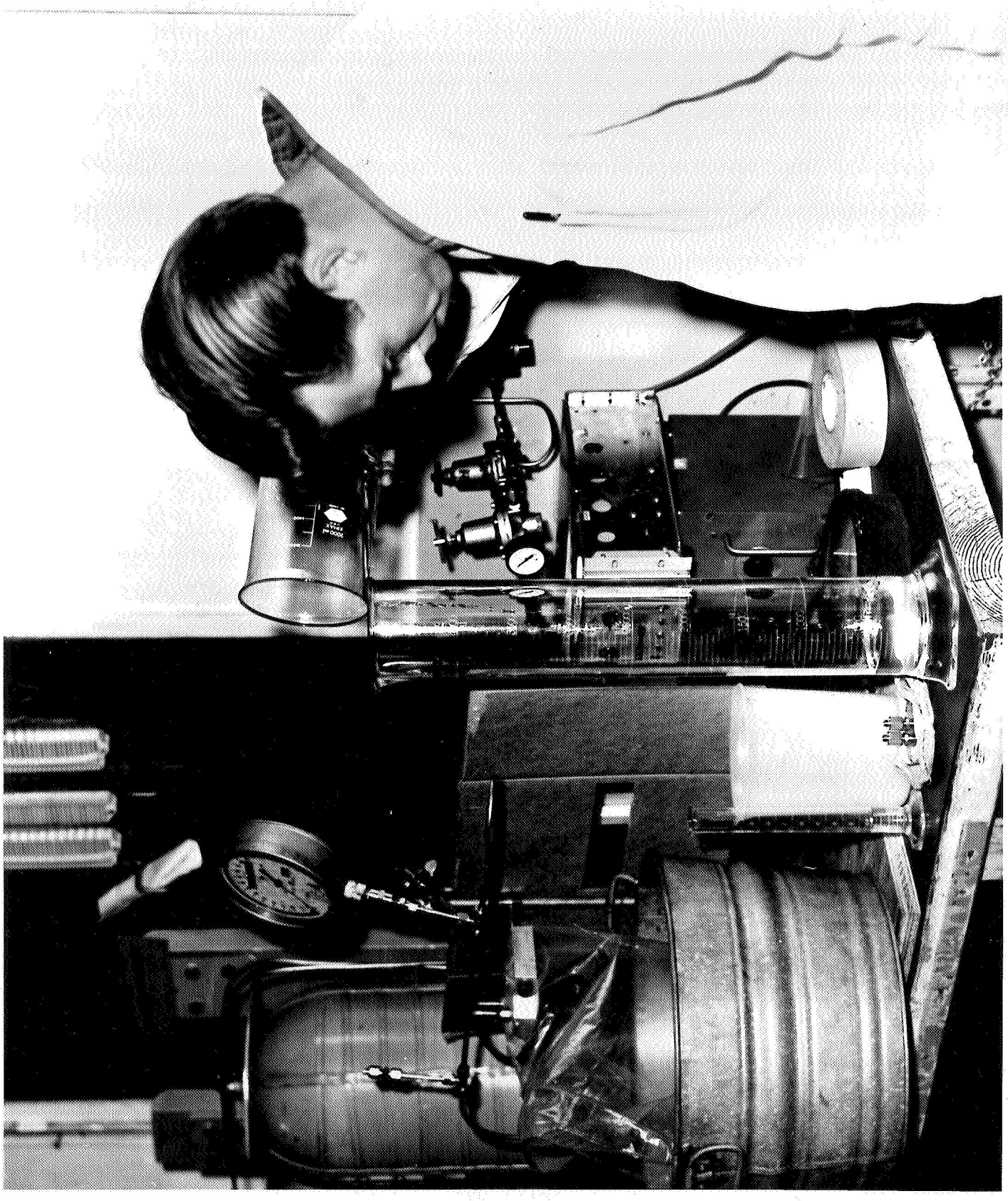

FIG. 5B. PHOTOGRAPH OF TEST CONFIGURATION

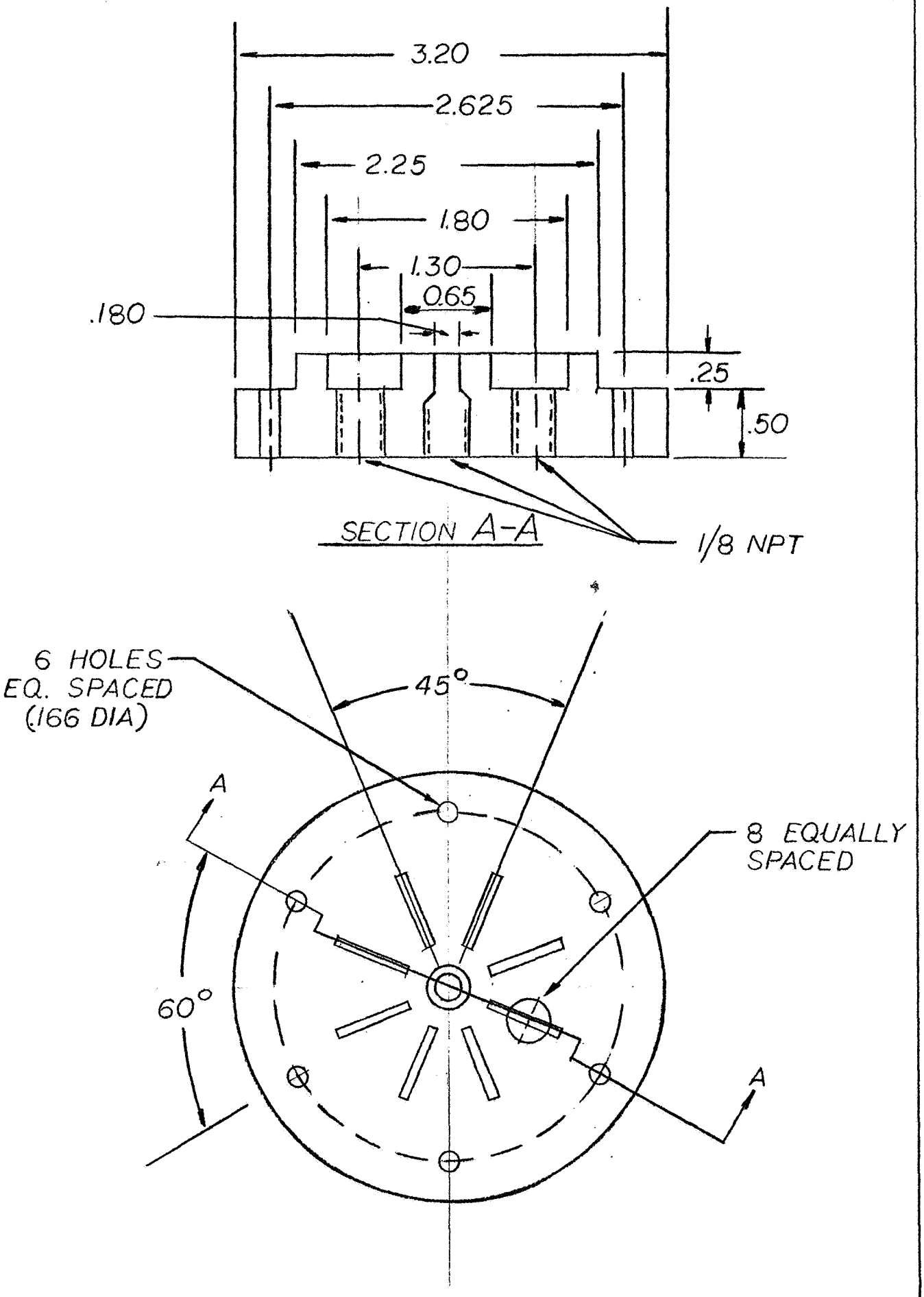

FIG. 6A. INJECTOR FRONT PLATE

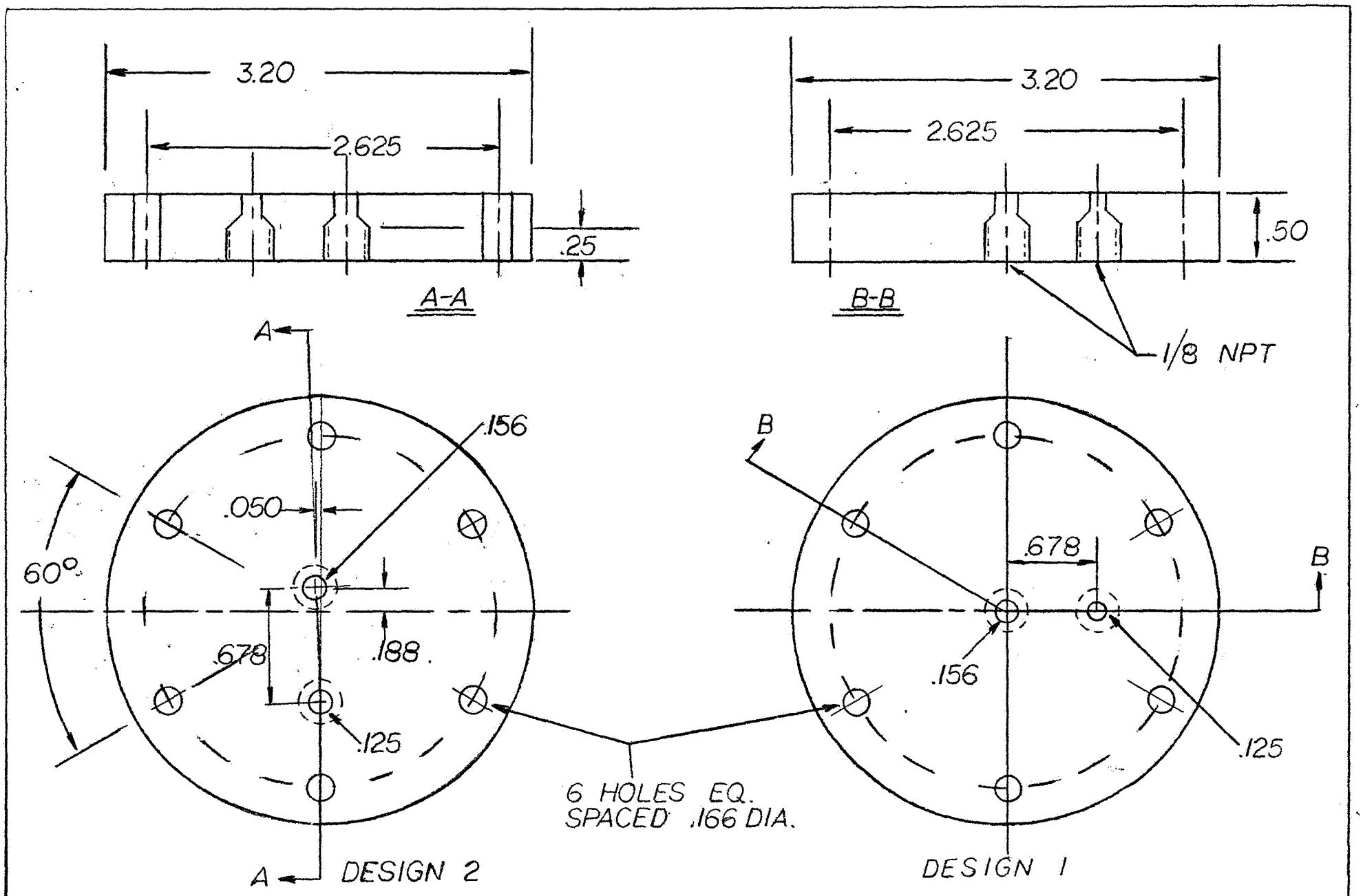

FIG. 6B. INJECTOR BACK PLATE

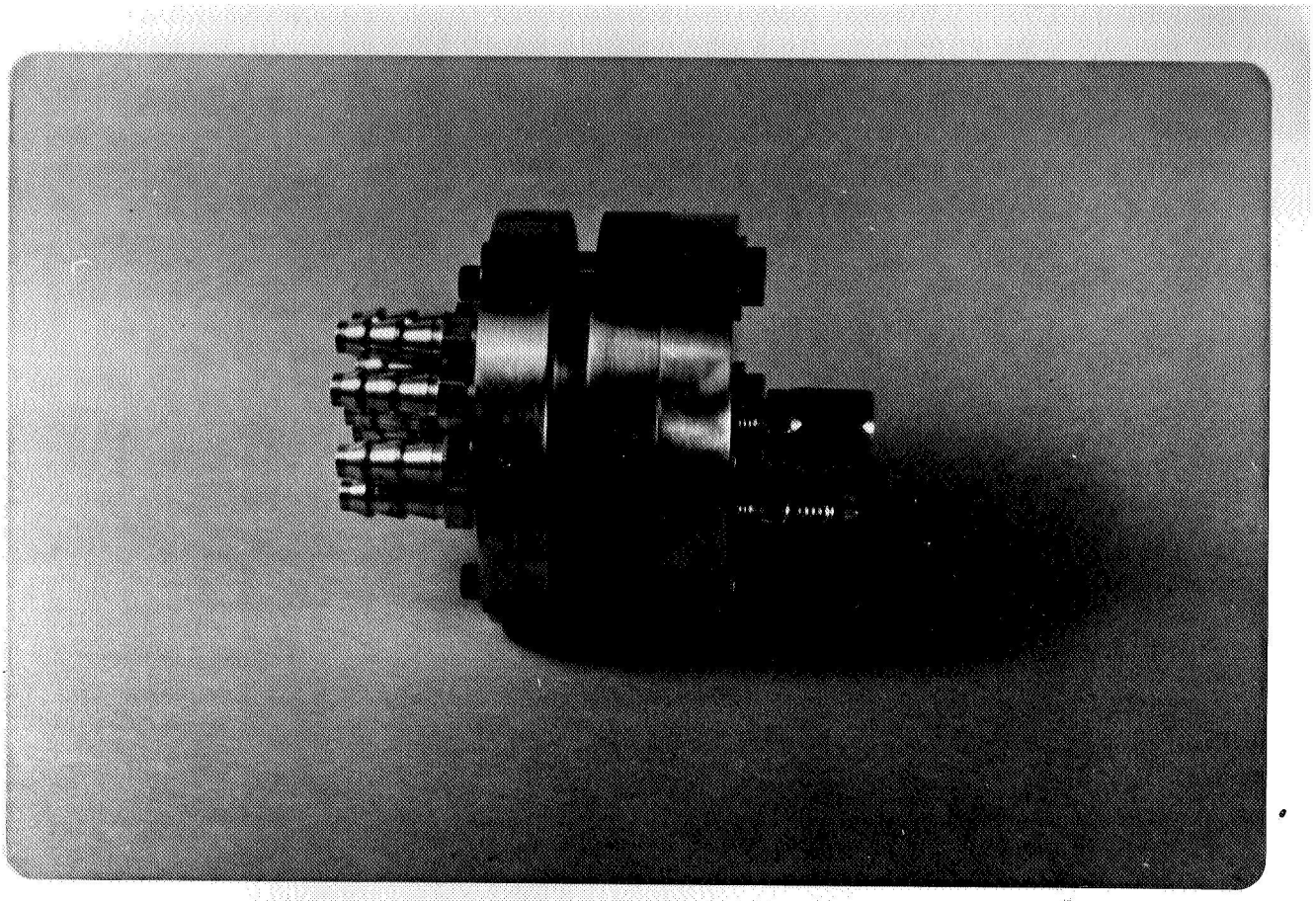

FIG. 7. PHOTOGRAPH OF THE INJECTOR WITH FRONT AND BACK PLATES MOUNTED

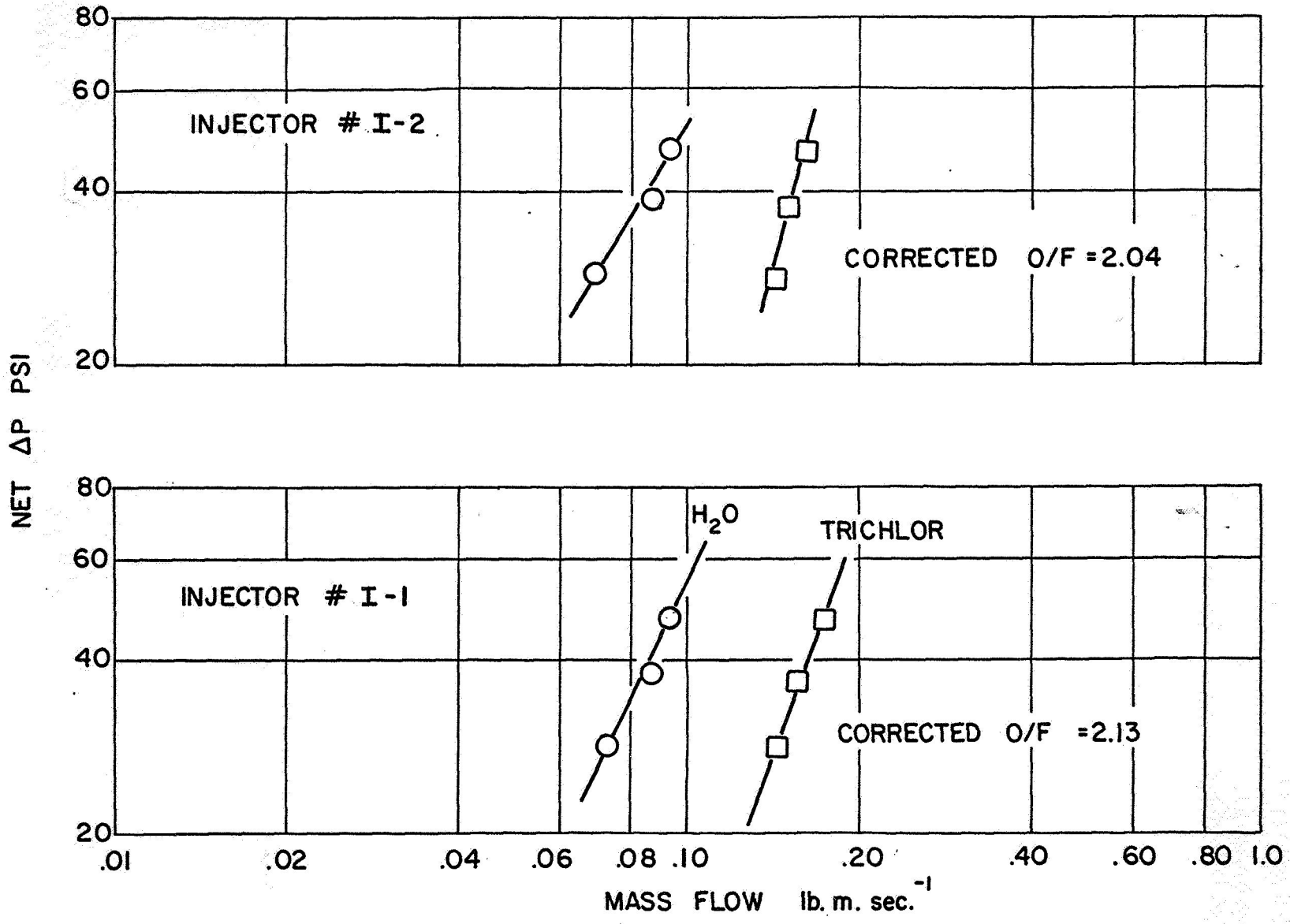

FIG. 8. REFERENCE FLUID MASS FLOW VS. PRESSURE DROP ACROSS INJECTORS SERIES I-1 AND I-2

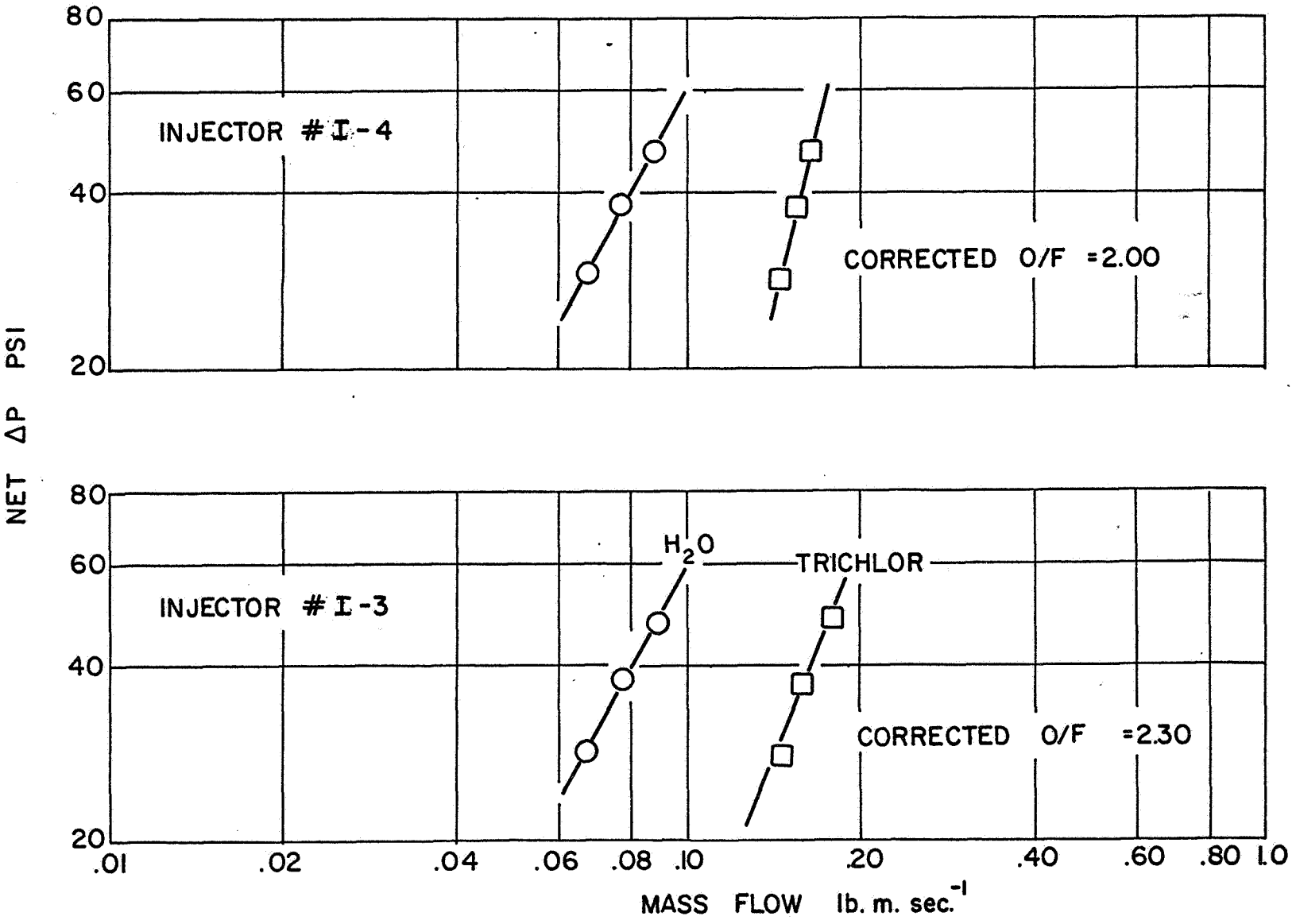

FIG. 8. REFERENCE FLUID MASS FLOW VS. PRESSURE DROP ACROSS INJECTORS SERIES I-3 AND I-4

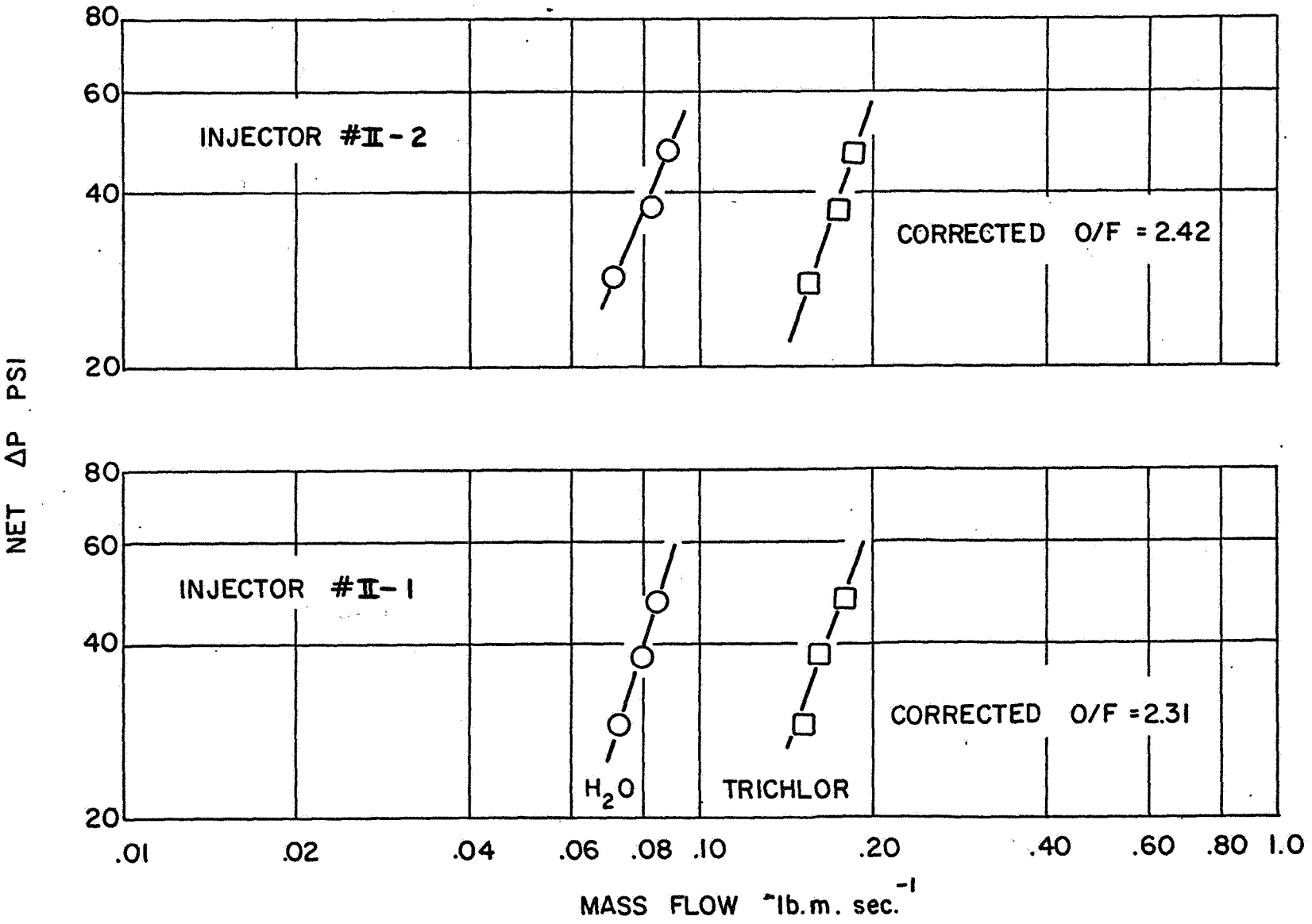

FIG. 9. REFERENCE FLUID MASS FLOW VS. PRESSURE DROP ACROSS INJECTORS SERIES II-1 AND II-2

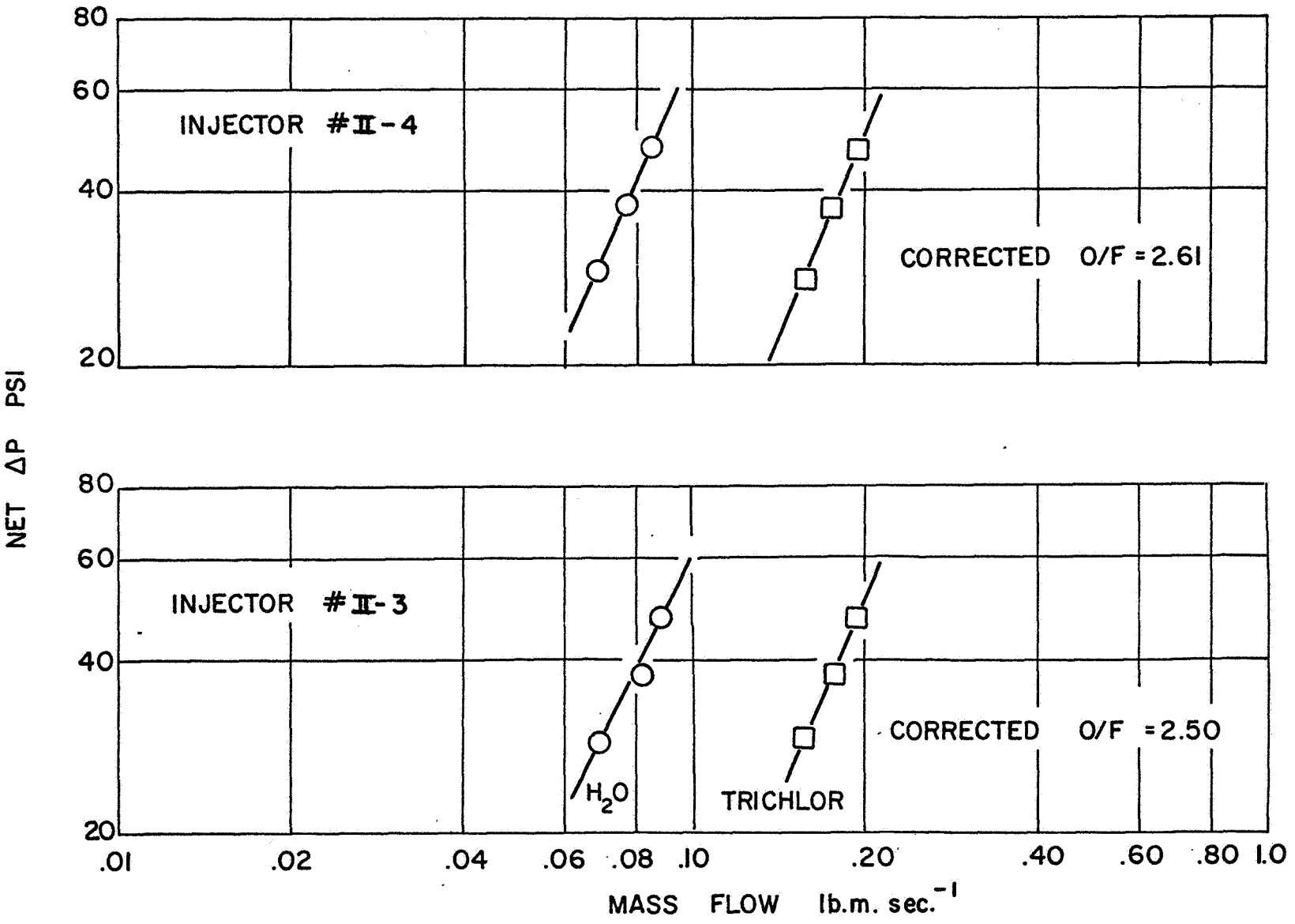

FIG. 9. REFERENCE FLUID MASS FLOW VS. PRESSURE DROP ACROSS INJECTORS SERIES II-3 AND II-4

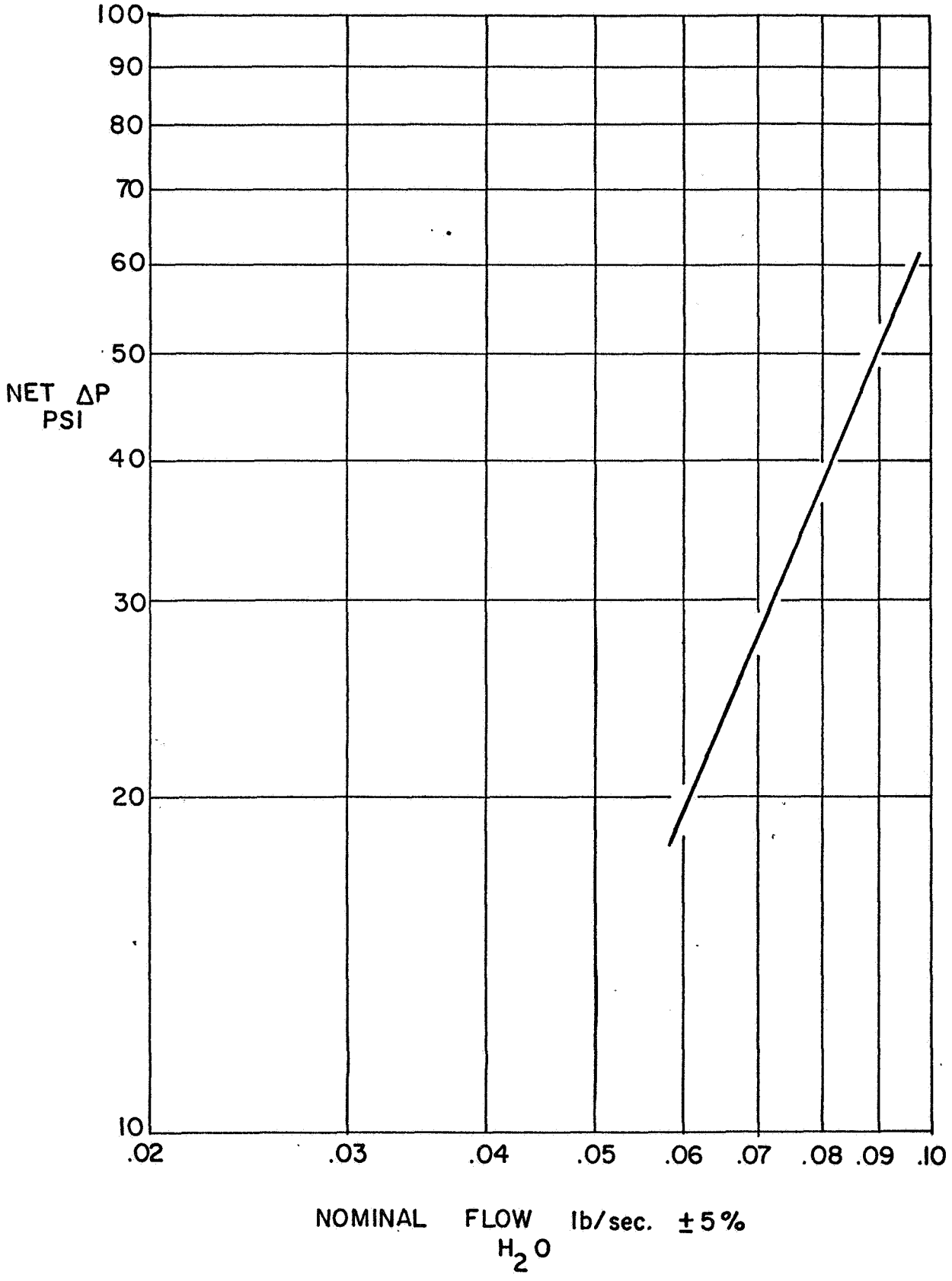

FIG. 10A. REFERENCE FLUID NOMINAL MASS FLOW VS. PRESSURE DROP ACROSS INJECTORS

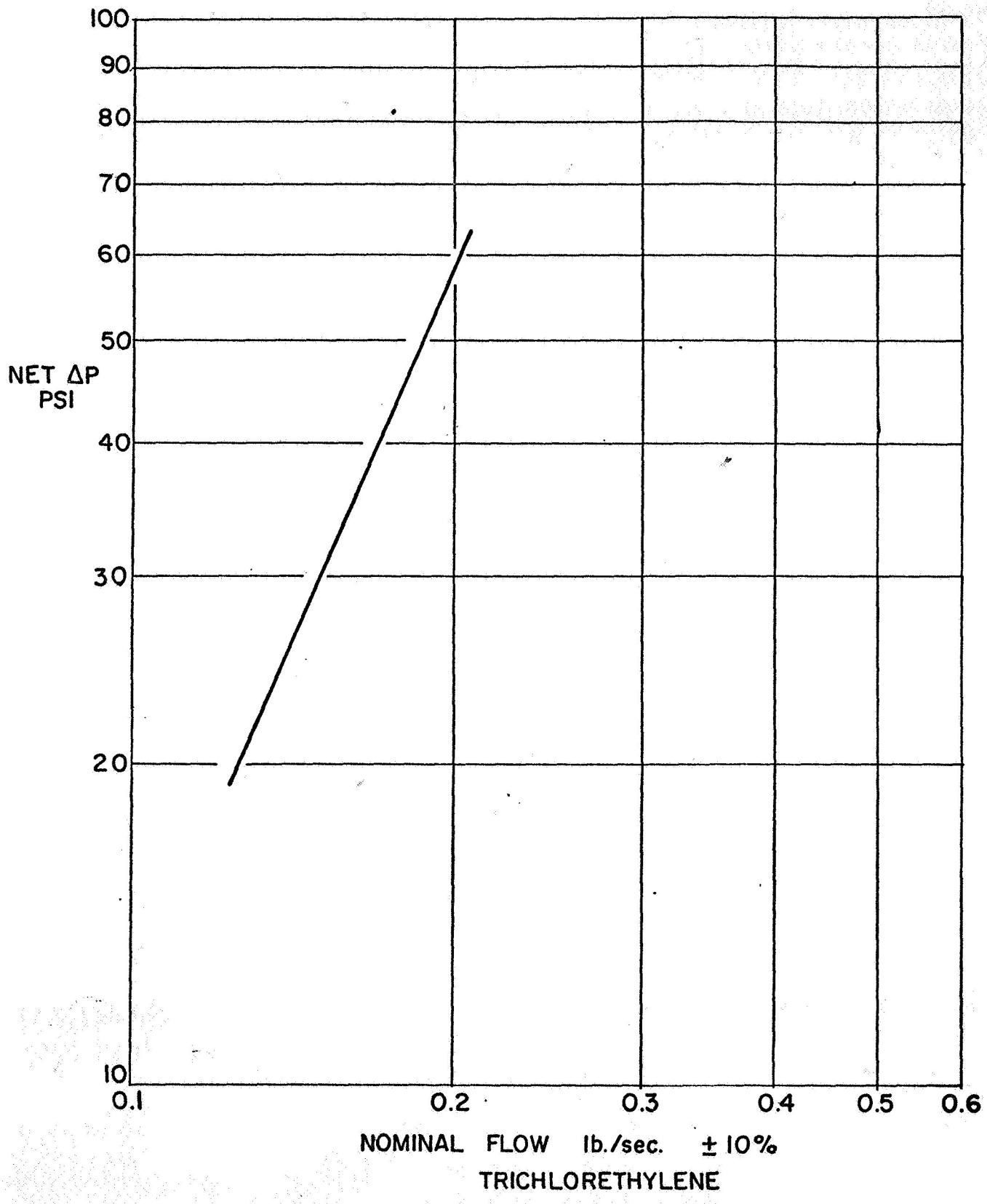

FIG. 10B. REFERENCE FLUID NOMINAL MASS FLOW VS. PRESSURE DROP ACROSS INJECTORS

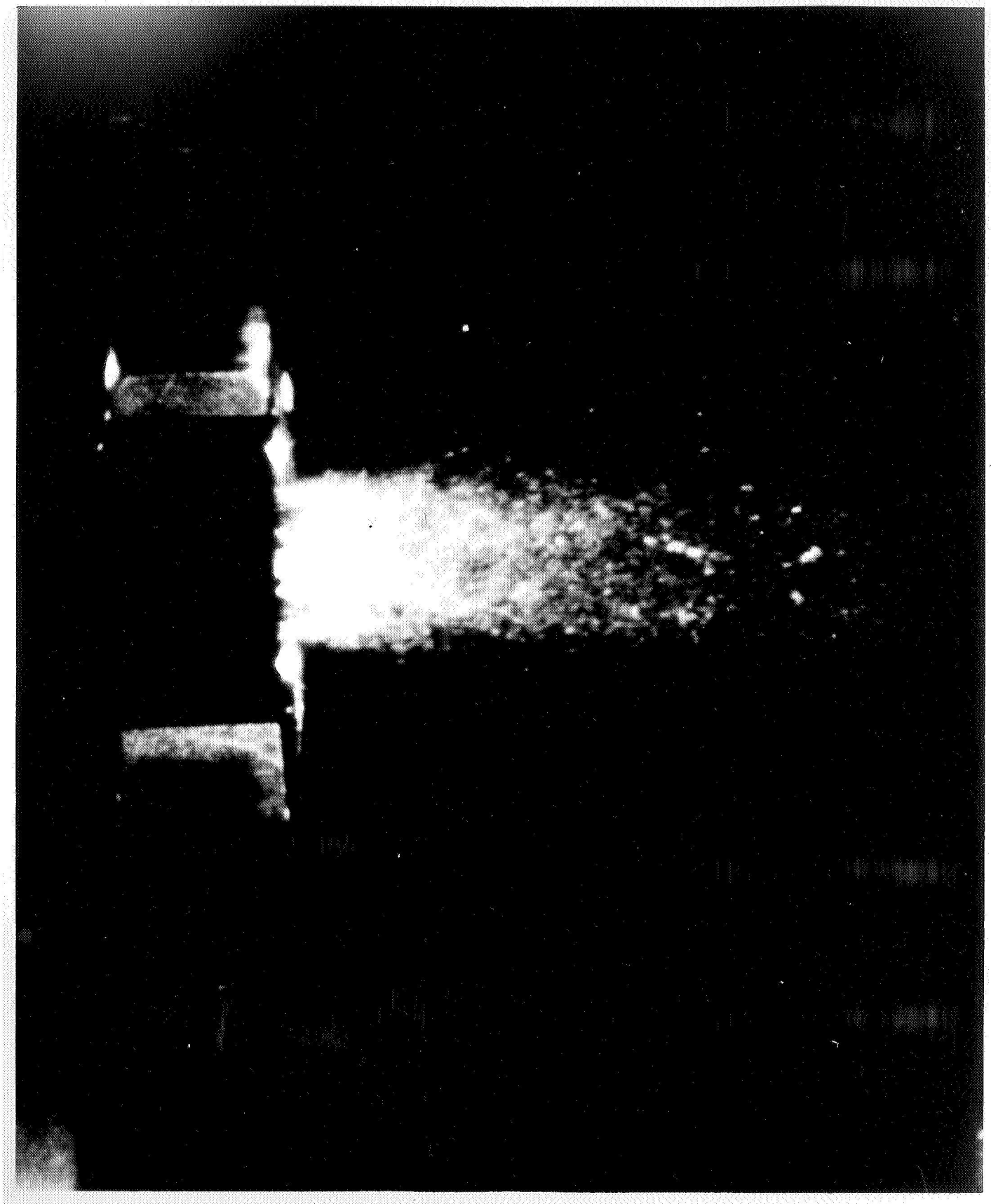

FIG. 11. PHOTOGRAPH OF INJECTOR II-2 FLOWING AT DESIGN POINT Δp=40 PSI

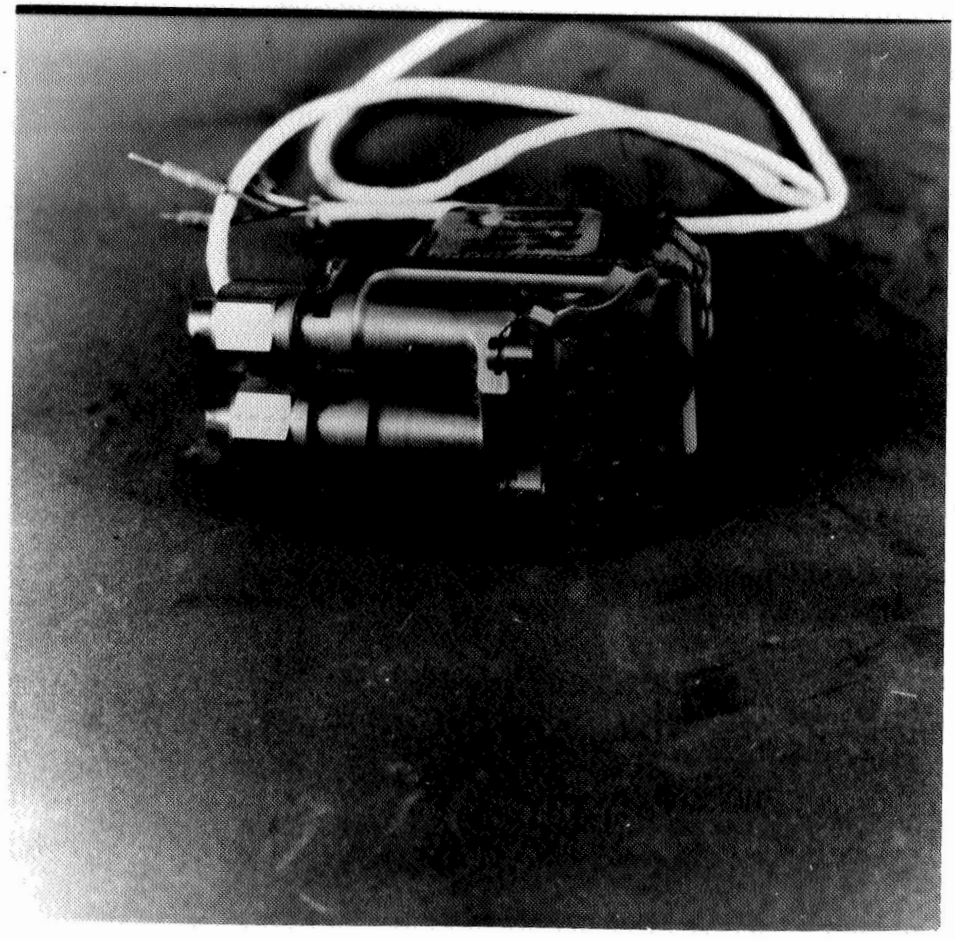

FIG. 12A. INJECTOR VALVE

FIG. 12B. INJECTOR VALVE OPERATION